RESEARCH

Open Access

Numerical Investigation of the Progressive Collapse of the Reinforced Concrete Wall-Frame Structures Considering the Soil–Structure Interaction

Seyed Ali Ekrami Kakhki[1], Ali Kheyroddin[2*] and Alireza Mortezaei[3]

Abstract

In this essay, the progressive collapse resistance of the reinforced concrete wall-frame structures was evaluated with and without considering the soil–structure interaction. The vulnerability of the frames against progressive collapse was investigated with the middle column removal scenario from the first story, based on the sensitivity index. To evaluate the effects of soil–structure interaction, the wall-frame structures along with the soil (hard soil) and foundation were simultaneously modeled in FLAC software and compared with the frames in Seismostruct software. The results showed that the sensitivity index decreased by considering the soil–structure interaction in the wall-frame structures. Afterward, a parametric study of the structures (foundation thickness) and substructures (soil types, soil densities, soil saturation conditions and soil layers) was performed. The results showed that with an increase in thickness of the foundation, the sensitivity index increased, and therefore, the condition of the structure would be more critical against progressive collapse. It was found that high groundwater levels in the subsoil can reduce its bearing capacity and lead to the damage to the structure. In addition, it was determined that by changing the substructure soil type from type 4 (Clay-MC) to type 1 (Rock), the use of layer 1 (SM) and layer 2 (SM-CL/ML (Very hard clay)-SM), and the soils with high density, the condition of the structures is better to prevent progressive collapse.

Highlights

- Progressive collapse was studied in RCSWs frames considering soil–structure interaction.
- A parametric study of structure and substructures was done on progressive collapse.
- Vulnerability of frames for progressive collapse was assessed by sensitivity index.

Keywords Progressive collapse, Vulnerability, Wall-frame structures, Soil–structure interaction, Sensitivity index

*Correspondence:
Ali Kheyroddin
kheyroddin@semnan.ac.ir
[1] Civil Engineering Department, Semnan Branch, Islamic Azad University, Semnan, Iran
[2] Department of Civil Engineering, Semnan University, Semnan, Iran
[3] Civil Engineering Department, Semnan Branch, Seismic Geotechnical and High Performance Concrete Research Centre, Islamic Azad University, Semnan, Iran

1 Introduction

Progressive collapse is described as the spread of an initial local failure from one element to another that may lead to a partial collapse of the structure or a large part of the building (Hou & Song, 2016; Kheyroddin et al., 2019; Rashidian et al., 2016; Yi et al., 2021). One typical structural failure with the following features is considered a progressive collapse. At first, the initial failure

Ekrami Kakhki *et al. Int J Concr Struct Mater*   (2023) 17:22

Page 2 of 24

should be localized, and should spread throughout the structure from one part to the other. The final structural failure should be disproportionate to the original failure (Adam et al., 2018; Kiakojouri et al., 2021; Kim & Choi, 2015; Trapani et al., 2020). The progressive collapse of the reinforced concrete (RC) structures can be caused by various types of abnormal loads, for example, gas explosions, bombs, fire, earthquakes, foundation failures, and construction or design errors (Mello et al., 2020; Petrone et al., 2016; Qian et al., 2021).

The collapses of the Ronan Point apartment building of London (1968), Skyline Towers Building in Virginia, USA in 1973, Civic Tower of Pavia in 1989, Campanile in Venice in 1902, Murrah Federal Building of Oklahoma City (1995), Khobar Towers of Saudi Arabia in 1996, the World Trade Center of New York (2001), and Windsor Tower of Spain in 2005 are the main examples of progressive collapses (Alshaikh et al., 2020; Kiakojouri et al., 2020; Masoero et al., 2010; Panahi & Zahrai, 2021; Russell et al., 2019; Seffen, 2008). Due to the importance of preventing the progressive collapse of structures, many efforts have been made in this field, which resulted in a series of design guidelines and specifications.

New guidelines and codes have been published to reduce the potential risk of progressive collapse of the structures, such as those provided by the U.S. Department of Defense (DoD,) and the General Service Administration (GSA,). According to these guidelines, there are several approaches to evaluate the progressive collapse of the structures, such as linear dynamic, linear static, nonlinear dynamic and nonlinear static approaches (Marjanishvili, 2004). The complexity of the analysis and the extensive time needed for computation make the nonlinear dynamic analysis an unsuitable method for progressive collapse analysis. Thus, in the present study, the nonlinear static analysis was used for evaluating the collapse behaviour of the frames.
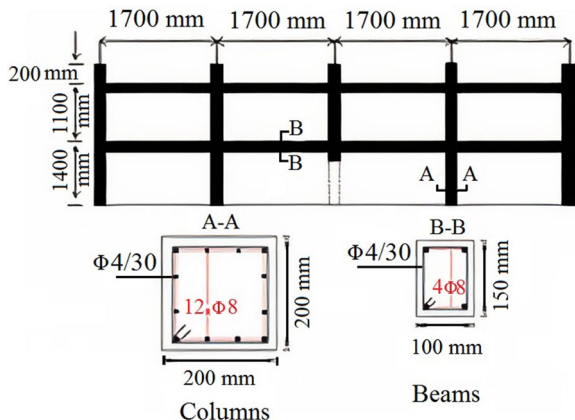

Fig. 1 Geometry and reinforcement layout of the Li experimental model utilized as reference (Li et al., 2016)
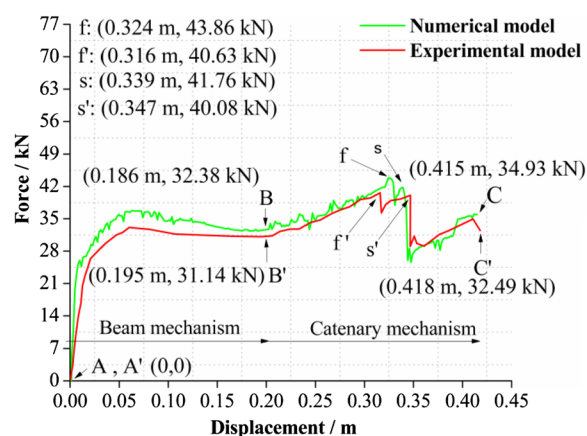

Fig. 2 Force–displacement curves of the numerical model and the experimental Li model (Li et al., 2016)

Although several studies have been performed to evaluate the progressive collapse resistance of reinforced concrete frames following the removal of a load-bearing element (Farahani et al., 2018; Francioli et al., 2021; Mucedero et al., 2020; Scalvenzi & Parisi, 2021), there have not been many studies in this field in RC frames with shear walls (Chehab et al., 2017; Esmaeilnia Omran & Hoseini Karani, 2018; Ren et al., 2015; Shayanfar & Javidan, 2017). Thomson et al. (2009) evaluated a simplified model for damage in squat RC shear walls. Bao and Kunnath (2010) investigated the progressive collapse of RC wall-frame structures following the sudden damage of a significant part of the shear wall. Faghihmaleki (2017) assessed the progressive collapse of RC-framed structures with shear walls under blast loading. Al-Ghalibi and Al-Hadithy (2018) reviewed RC walls under seismic effects, and progressive collapse. Liu et al. (2018) proposed an extreme point symmetric mode decomposition (ESMD) method to perform the stability analysis in the progressive collapse of an RC shear wall-frame building model. Elmagbool et al. (2021) assessed the progressive collapse analysis of shear wall-framed structures considering the various soil profile types.

In the progressive collapse analysis of the structures, the effects of soil–structure interaction (SSI) are not usually considered, and the structure is evaluated as a solid foundation structure (Azimi & Molaei Yeznabad, 2020; Fathi et al., 2020; Güllü & Karabekmez, 2017; Patel & Shah, 2017). Considering the SSI makes the analysis a time-consuming process, but using it leads to more realistic results than conventional methods. Soil–structure interactions can play a very effective role in assessing the vulnerability of buildings to progressive collapse. By considering SSI, the estimated forces on the structure members are different from the conventional method of analysis (Anvarsamarin et al., 2020; Behnamfar &

Banizadeh, 2016; Karapetrou et al., 2015; Khatibinia et al., 2013; Payganeh & Mortezaei, 2020). The numerical methods to study the effect of SSI can be classified as the direct approach and the substructure approach (Cavalieri et al., 2020; Li et al., 2014; Mourlas et al., 2020). The first method is the direct approach in which soil, foundations and structures are included in a single model and examined as a complete system. In this approach, the vulnerability of the foundation, superstructure, and soil in progressive collapse can be accurately investigated (Far & Flint, 2017). In the substructure approach, the soil–structure interaction is considered as two separate systems, and the coupling of subdomains is done by impedance functions. In this approach, the springs are incorporated

Table 1 Specifications of the frames

Yield strength of longitudinal reinforcing rebars	234 MPa
Yield strength of transverse reinforcing rebars	234 MPa
Concrete mean compressive strength	41.3 MPa
Dead loads	4 kN/m^2
Live loads	4 kN/m^2
The bedrock peak ground acceleration	0.24 g
Ground type	B-type
Behaviour factor	5.85

to demonstrate the foundation and adjacent soil (Pitilakis & Clouteau, 2010). The substructure method is applied, assuming the linear behaviour of soil and structure. The
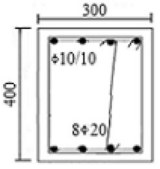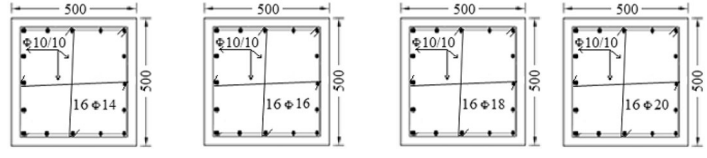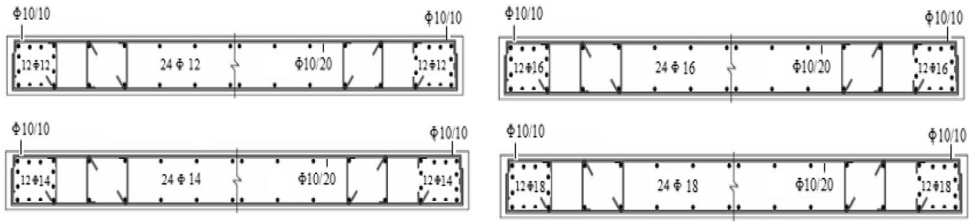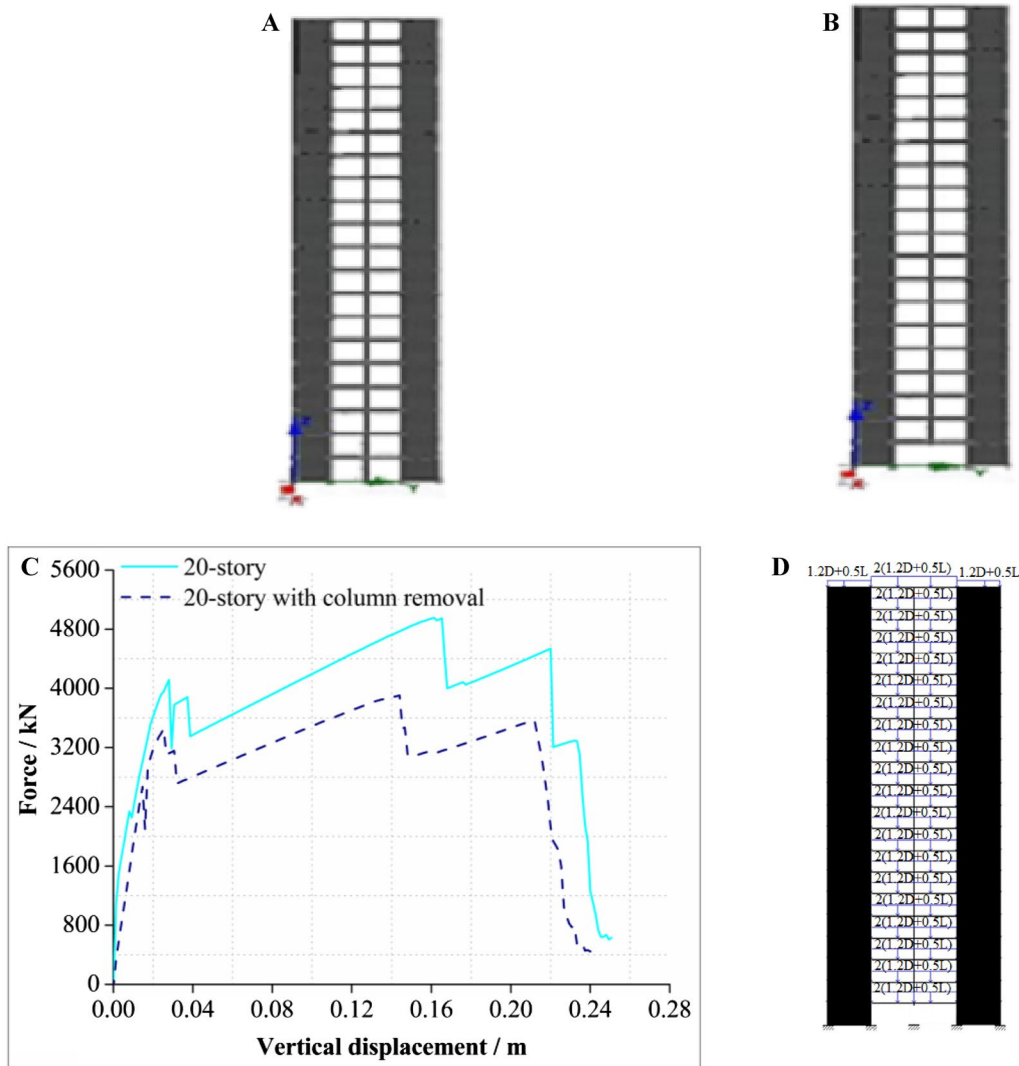

Fig. 3 Numerical models of the 20-story RCSWs frames **A** without and **B** with the middle column removal in SeismoStruct software, **C** Force–displacement curves of the frames with and without column removal, **D** Loading shape of the frames with column removal

Table 2 Dimensional specification and reinforcement layout of beams, columns and RCSWs of the 20-story frames

Beams			Columns		
Size (depth × width) (mm²)	Longitudinal reinforcement	Transverse reinforcement	Size (depth × width) (mm²)	Longitudinal reinforcement	Transverse reinforcement
400 × 300	8 Φ 20	Φ10/100 mm	500 × 500	16 Φ 14	Φ10/100 mm
				16 Φ 16	
				16 Φ 18	
				16 Φ 20	

RCSWs				
Size (wall width × thickness of section edges × width of section edges × thickness of section core) (mm)	Longitudinal reinforcement corner 1 and 2	Longitudinal reinforcement middle	Transverse reinforcement upper and lower	Transverse Reinforcement middle
3000 × 250 × 250 × 250	24 Φ 12	24 Φ 12	Φ10/100 mm	Φ10/200 mm
	24 Φ 14	24 Φ 14		
	24 Φ 16	24 Φ 16		
	24 Φ 18	24 Φ 18		

real subsoil behaviour is nonlinear (Jarernprasert et al., 2013). In the direct approach, it is possible to perform the nonlinear analysis accurately. Therefore, it is more accurate for the dynamic analysis of soil–structure systems (Far, 2019).

Despite the advantages of using three-dimensional (3D) modeling of structures in the investigation of progressive collapse, the use of 3D models has some disadvantages, such as the time-consuming analysis, the possibility of not specifying all the parameters during the design process, more difficult control of the results compared to the two-dimensional (2D) model and the probability of the apparent accuracy of the results. The use of two-dimensional models of the RC frames enables a more practical comparison of the experimental and numerical results, because three-dimensional experimental models require advanced equipment and special equipped laboratories.

This is while two-dimensional experimental models are tested in most laboratories with common equipment. Furthermore, from a practical point of view, 3D modeling of soil, foundation and structure in the laboratory in real dimensions is very difficult, and scaling the soil may lead to the different results than the real model. Therefore, in many articles, the experimental and numerical results of two-dimensional models are examined (Elsanadedy & Abadel, 2022; Lin et al., 2022; Qian et al., 2021; Tao & Huang, 2022).

In this novel work, the progressive collapse resistance of the two-dimensional (2D) reinforced concrete wall-frame structures was investigated with considering the SSI. For simplicity, reinforced concrete frames with concrete shear walls are named as RCSWs frames. At first, the RCSWs frames were modeled in SeismoStruct software. Afterward, the frames accompanied by foundation

and soil were simulated in the 2D fast Lagrangian analysis of continua (FLAC) finite-difference software using the direct approach and verified with the corresponding models in SeismoStruct software. To assess the progressive collapse of the RCSWs frames, a nonlinear static pushdown analysis was performed. The vulnerability of the frames was evaluated following the middle column removal from the first story based on the sensitivity index (SI). Afterward, the effects of different parameters of the progressive collapse of the 20-story RCSWs frames, including soil layers, soil types, soil density, foundation thickness, and soil saturation conditions, were investigated. Furthermore, the vulnerability of the frames with and without considering the SSI was compared with each other.

2 Modeling and Analysis
2.1 Reference Specimen
To validate the inelastic macro model investigated in this work, the experimental specimen of Li et al. (2016) was utilized as a reference. The geometric specification of the reference specimen was as follows: the centre-to-centre (S) of the columns was 1.70 m. The inter-story heights of the first and second stories were 1.35 and 1.10 m, respectively. The cross sections (height to width) of the

beams were 150×100 mm^2, and those of columns were 200×200 mm^2. The transverse reinforcement of beams and columns were 2-leg Φ4 and 4-legΦ 4, respectively. The longitudinal rebars of beams and columns were 4Φ8 and 12Φ8, respectively. The distance of stirrups in beams was 30 mm at both end zones, whereas in columns, it was 33 mm at the base of the ground-floor columns and 50 mm everywhere else. The main features of the reference 2-story frame with 4-bay in a 1/3 scale and its reinforcement layout are represented in Fig. 1.

2.2 Numerical Modeling and Verification
After simulating the experimental Li specimen in SeismoStruct software, the numerical model was verified.

To model the RCSWs frames in Seismostruct software, first the material specifications of rebars and concrete are defined in the preprocessor menu. Afterward, the sections of the beams, columns, and shear walls are defined in the section menu. In this section, the material properties are specified. Then, in the element menu classes, the element type infrmFBPH is selected. Afterward, the desired nodes are selected, and the points of the walls are connected in the element connectivity menu. Load strain, concrete strain, and shear are defined in the performance criteria section. Then, the pushdown analysis is performed.
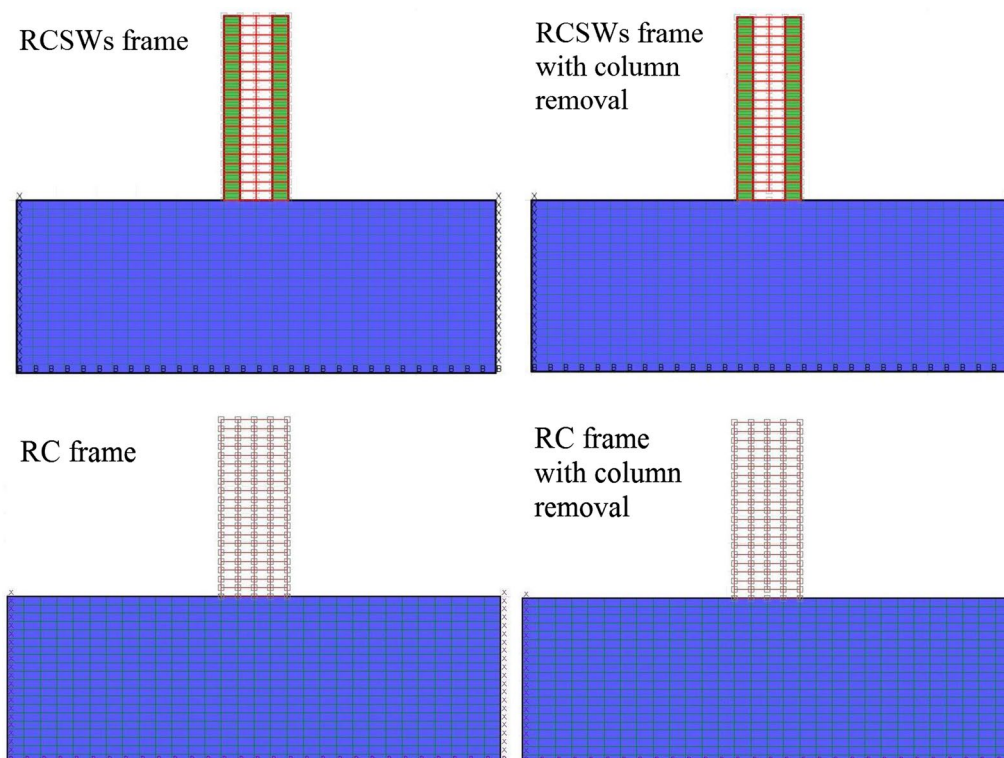

Fig. 4 Numerical models of the 20-story RCSWs and RC frames with and without column removal in FLAC software

Shear walls with the thickness of 25 cm, the length of 3 m and the height of 3.2 m were designed. To consider the non-linearity of the material, the cross-sectional area of the member is divided into a certain number of fibers, and this division is observed throughout the member length. Then, the cross-sectional stress–strain diagram of the member is obtained by integrating the stress–strain diagram of different fibers. To consider the non-linearity of the materials, 6 integration cross sections have been used with the Gauss–Lobatto formulation at the height of the wall, with the number of 150 fibers for each cross section.

The single inelastic force-based plastic-hinge frame elements (infrmFBPH) with 400 section fibres and 16.67% plastic hinge length were utilized for modeling the beams and columns. A static method and a hybrid solution procedure between the classic and modified Newton–Raphson approaches were used for the finite element (FE) analysis. 10^{-3} was considered the threshold for the convergence criterion based on the assumed displacement/rotation. The displacement rate was determined to be at least 0.1 mm per step. The model nodes were all restrained against the out-of-plane displacements, the frame's vertical axis, and rotation around the in-plane horizontal axis. Geometrical nonlinearities, caused by the large displacements/rotations and P-Delta effects, were incorporated in accordance with a total corotational formulation. The inelastic behaviour of concrete was simulated using the uniaxial uniform confinement model proposed by Mander et al. (1988). The stress–strain relationships were utilized in accordance with Martinez-Rueda and Elnashai (1997) as follows:

$$f_c = \frac{f_{cc}' x r}{r - 1 + x^r} \tag{1}$$

f_c defines the longitudinal compressive concrete stress:

$$f_{cc}' = k f_{co}' \tag{2}$$

k refers to the confinement factor. f_{cc}' and f_{co}' are the compressive strength (peak stress) of the confined concrete and the unconfined concrete strength, respectively:

$$x = \varepsilon_c / \varepsilon_{cc} \tag{3}$$

ε_c is related to the longitudinal compressive concrete strain and ε_{cc} is the strain at f_{cc}':

$$\varepsilon_{cc} = \varepsilon_{co} \left[1 + 5 \left(\frac{f_{cc}'}{f_{co}'} - 1 \right) \right] \tag{4}$$

ε_{co} refers to the strain at unconfined stress f_{co}:

$$r = \frac{E_c}{E_c - E_{sec}} \tag{5}$$

E_c is the initial modulus of concrete elasticity, and E_{sec} defines the secant modulus of concrete elasticity at peak stress:

$$E_c = 5000 \sqrt{f_{co}'} \tag{6}$$

$$E_{sec} = \frac{f_{cc}'}{\varepsilon_{cc}} \tag{7}$$

Comparing the force–displacement curves of the experimental Li model utilized as a reference specimen and the numerical model obtained from the pushdown analysis showed that there is a good agreement between the results of the experimental and numerical models (Fig. 2).

Two main mechanisms, including the beam mechanism and the catenary action (CA) mechanism are known for the progressive collapse resistance of the structures (Kai et al., 2019). The beam mechanism is related to the flexural capacities of the beams and their compressive arch action (CAA). The areas related to these mechanisms are displayed in Fig. 2. A refers to the initial point, B is the transition point between the beam and the catenary mechanisms, and AB is the stage related to the beam mechanism. After point B, due to the catenary action mechanism, the load capacity increases with increasing the vertical displacement until the first rebar fracture. Point C corresponds to the maximum vertical displacement, and stage BC refers to the catenary action. f and s points refer to the first and second rebar fracture in the numerical model, whereas f' and s' are the corresponding points in the experimental model. A', B' and C' are the initial, transition, and maximum vertical displacement points in the experimental model.

The maximum load-carrying capacity of the numerical model before the first rebar fracture at the end of the beams (43.86 kN) shows a difference of about 7.4% compared to the experimental model (40.63 kN). The displacement corresponding to the first rebar fracture in the numerical model (324 mm) shows a difference of about 2.47% compared to the experimental model (316 mm). In addition, there is a difference of about 2.3% in the displacement of the second rebar fracture for the numerical (339 mm) and the experimental (347 mm) models.

3 Development of the Numerical Model
As the numerical model was simulated according to the experimental Li specimen (Li et al., 2016) in Seismo-Struct software, the 2D model was developed. A 20-story
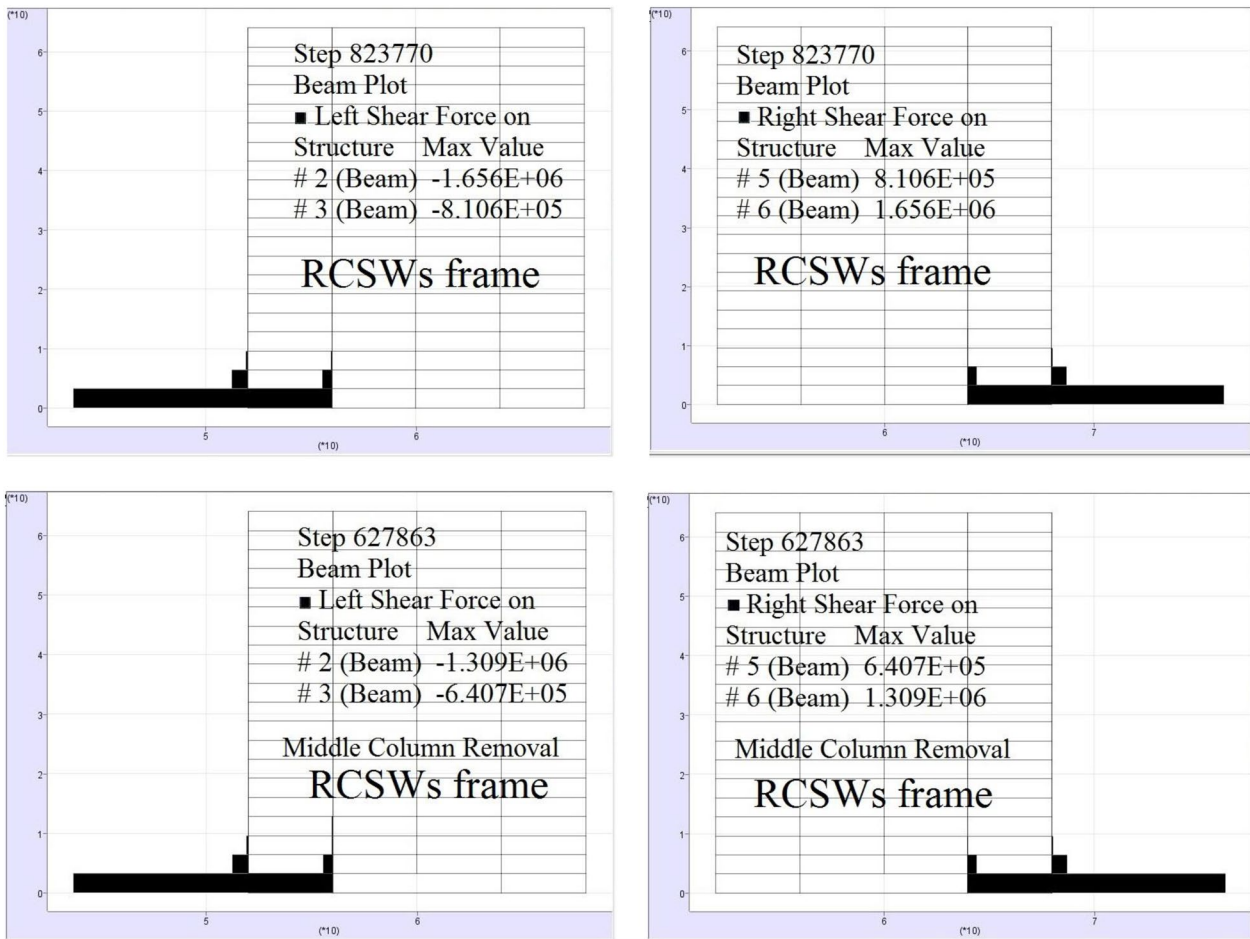
Fig. 5 Total base shear of the RCSWs frames with and without middle column removal

Table 3 Redistribution of the imposed loads and Y-displacement in the 20-story RCSWs frames with the middle column removal

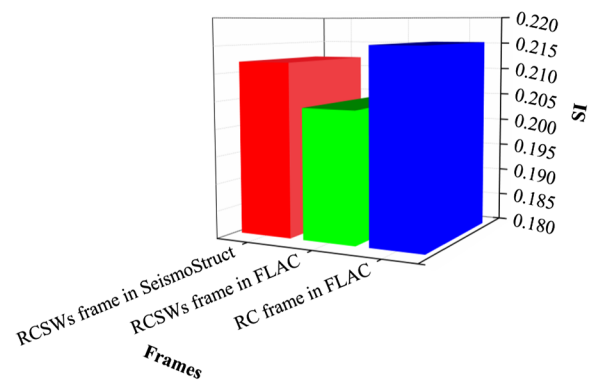| Software			Discrepancy (%)
SeismoStruct	y-disp$_0$ (m)	0.0671	
	y-disp$_{damage}$ (m)	0.0583	
	λ_0 (kN)	4954.893	
	λ_{dmage} (kN)	3903.981	
	SI	0.212	
FLAC	y-disp$_0$ (m)	0.0682	1.64
	y-disp$_{damage}$ (m)	0.0596	2.23
	λ_0 (kN)	4901.2	1.08
	λ_{dmage} (kN)	3899.4	0.12
	SI	0.204	3.77

Fig. 6 Plot of the sensitivity index of RCSWs and RC frames in FLAC software, and RCSWs frame in SeismoStruct software

reinforced concrete frame with shear walls with a story height of 3.2 m and a span length of 3 m was modeled with and without removing the middle column (Fig. 3A and B). The specifications of the frames are shown in Table 1. The structures were designed with the criteria of structures with medium ductility class. The live and dead loads for the earthquake-resistant structures were utilized according to the European seismic provisions (). The reinforcement layout and the dimensional specifications of columns, beams and RCSWs of the frames are shown in Table 2. The resistance capacity of RCSWs frames against progressive collapse was evaluated using a nonlinear static pushdown analysis with the middle column removal from the first story. The force–displacement curves of the 20-story RCSWs frames with and without removing the middle column are represented in Fig. 3C. Loading was performed according to the DoD guidelines.

The gravity load combination applied to the beams adjacent to the removed column is represented by Eq. (8). In the nonlinear static analysis method, a magnification factor of 2 is used to consider the dynamic effects of column removal.

$$Load = 2[1.2D + 0.5L] \tag{8}$$

According to the DoD guidelines, the dynamic amplification factor is not recommended for dynamic analysis. The following equation is used for the load combination applied to the beams adjacent to the removed column in the linear and nonlinear dynamic analysis:

$$Load = [1.2D + 0.5L] \tag{9}$$

L refers to the floor live load, and D is ascribed to the dead load.

According to the UFC 4-023-03, Eq. 8 is used for Force-Controlled actions. The increased gravity load combination in Eq. 8 is applied to those bays immediately adjacent to the removed element and at all floors above the removed element. Gravity Loads for floor areas away from removed column is applied according to Eq. 9 (Fig. 3D).

In the progressive collapse assessment of RCSWs frames, the sensitivity index (SI) was utilized as follows (Jiang et al., 2020; Kwon & Kim, 2014):

$$SI = (\lambda_0 - \lambda_{damage})/\lambda_0 \tag{10}$$

In this regard, λ_0 is the maximum load-carrying capacity of the structure before removing the column, and λ_{damage} is the maximum load-carrying capacity of the structure after the column removal. According to the above formula, when the load-carrying capacity of the structure changes slightly by removing a member, the

Table 4 Redistribution of the imposed loads in the 20-story RCSWs frames with various foundation thicknesses in FLAC software

Thickness of foundation (cm)	λ_0 (kN)	λ_{damage} (kN)	SI
180	5147.8	4162.8	0.1913
190	4933.6	3948.6	0.1997
200	4660.4	3719	0.2019
210	4451.4	3546.2	0.2033

structure's sensitivity to that member can be ignored, and the removal of that member is less important in maintaining the load-carrying capacity of the structure. On the other hand, removing a member with SI = 1 causes the collapse of the whole structure or a part of it. Such a member is considered a key member or a vulnerable point of the frame. If a member is removed, the higher the sensitivity index, the lower the load-carrying capacity of the structure. Therefore, the element with the highest sensitivity index will be the critical element of the structure.

In this research, the progressive collapse of the 20-story RCSWs frames was investigated with the column removal scenario. The vertical increasing load was applied to the upper node of the removed column. By increasing the amount of force, applied to the structure, and consequently increasing the stresses, bending plastic hinges were created in the beams, shear wall base, and columns. The hyper-elastic behaviour of the structure is one of the most important inherent characteristics of its members, which can be checked by placing plastic hinges in the structure members. In this research, infrmFBPH has been used to define plastic hinges, where plastic hinges are at two ends of the member (beams and columns), that is, only two ends can be nonlinear. In fact, after removing the column, plastic hinges are first formed at the two ends of the beams. Then, by creating the plastic hinges at the shear wall base and the columns, the structure is completely destroyed. With the formation of the plastic hinges at the wall base, the wall is destroyed.

The influence of soil–structure interaction on the progressive collapse of RCSWs frames was evaluated following the column removal. For this purpose, soil, foundation and RCSWs frames were simultaneously modeled in FLAC software with and without column removal (Fig. 4). To evaluate the effect of RCSWs on the progressive collapse of the frames, the RC frames without RCSWs were also modeled with and without column removal in FLAC software (Fig. 4). The structural components were modeled using the beam structural elements, and the soil medium was modeled using the two-dimensional plane-strain grid consisting of quadrilateral
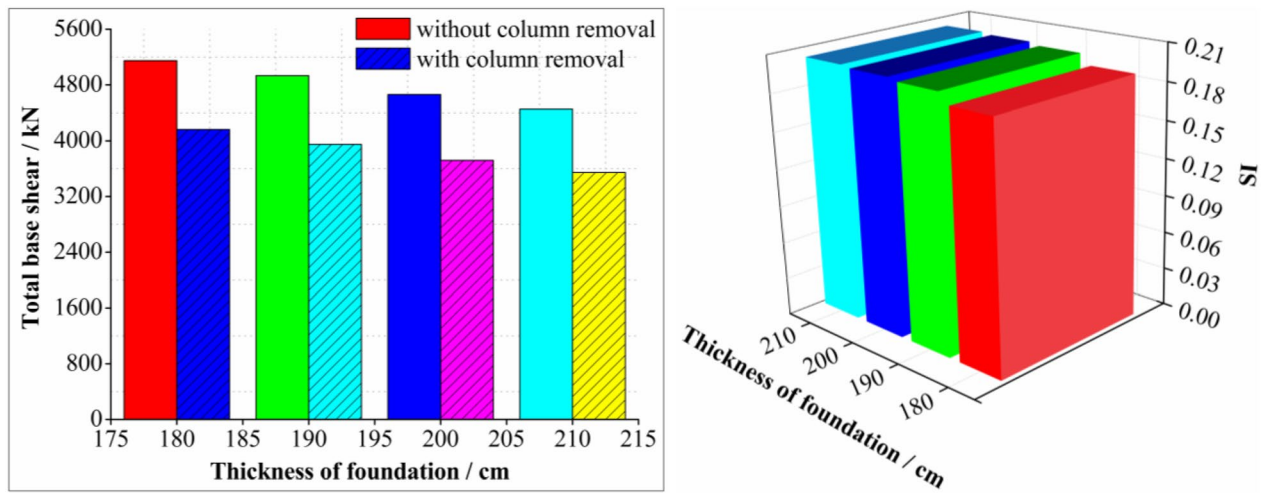
Fig. 7 Total base shear with and without column removal and the plot of the sensitivity index for different thicknesses of foundation

elements. The beam structural elements are two-nodded, finite elements with six degrees of freedom in each node, with three rotational and three translational components. Rigid boundary condition was assumed for the bedrock, and quiet (viscous) boundaries were considered as the lateral boundaries of the soil medium. To simulate the nonlinear behaviour of the soil medium, the Mohr–Coulomb model was utilized as a constructive model.

The distance of the lateral and lower boundaries was chosen based on the following notes. The lateral boundaries should be large enough to completely contain the stress bubble, and the stress due to the load of the structure in the bottom of the model should be less than 10% of the stress under the foundation. In addition, the lateral boundaries should be large enough to accommodate the possible rupture wedge in the limit state. For this purpose, it is suggested to select the width of the model (B) in the range of 3 to 5 times the dimensions of the structure (D) on each side. In the case of the environment with high damping, the lower limit is recommended, and in the environment with low damping, the higher limit is suggested. It is also recommended that in thin structures with a higher h/D ratio than usual (h is the height of the structure), the width of the model be greater than the above mentioned value.

Regarding the lower boundaries, it is recommended that the lower boundary be placed at a depth, where the soil of the lower layer has more stiffness than the upper layers, and the soil depth continues to the layer, where the shear wave speed is more than 750 m/s. It is recommended to continue the depth of soil until the hardness of the bottom layers is at least 10 times higher than the surface soil layers. Therefore, soil depth between 30 and 70 m is recommended (Lysmer & Kuhlemeyer, 1969; Rahmani et al., 2016; Wolf, 1985).

In this research, considering that the damping of the structure is at the low level of normal structures and the dimensions of the investigated structures (D) are 12 m, the width of the model was considered to be 54 m on each side. Therefore, the total width of the substructure soil model was considered to be 120 m. In addition, due to the use of tall structures, the depth of the bedrock was chosen to be 60 m. Since this is a plane strain problem, the width of the strip foundation was utilized for calculating the inertia moment of the concrete element.

Bond of reinforcing bars to the surrounding concrete influences the behaviour of the reinforced concrete structures in many ways. The bond actions are comprised of an adhesive bond, a frictional bond, and a shear bond. In the deformed bars, the bond resistance capacity is mainly governed by the mechanical interlocking action (Sivaselvan & Reinhorn, 1999). The generally accepted values ranging between 0.05 and 0.15 represent a good compromise for the relative rib area, in terms of ultimate bond strength and splitting ability, and so forth.

In this work, the modified Ikki equation (Ikki & Kiyomiya, 1996; Ikki et al., 1996) was utilized for the bond-slip between concrete and steel rebar as follows:

$$\tau_b = k \times f_c'^{2/3} \times \left\{ 1 - \exp\left[-4500 \left(\frac{S}{d_s} \right)^{1.45} \right] \right\}^{0.5}$$
$$\times \exp\left[-5 \left(\frac{S}{d_s} \right) + 5.5 f_R^{0.9} \right]$$
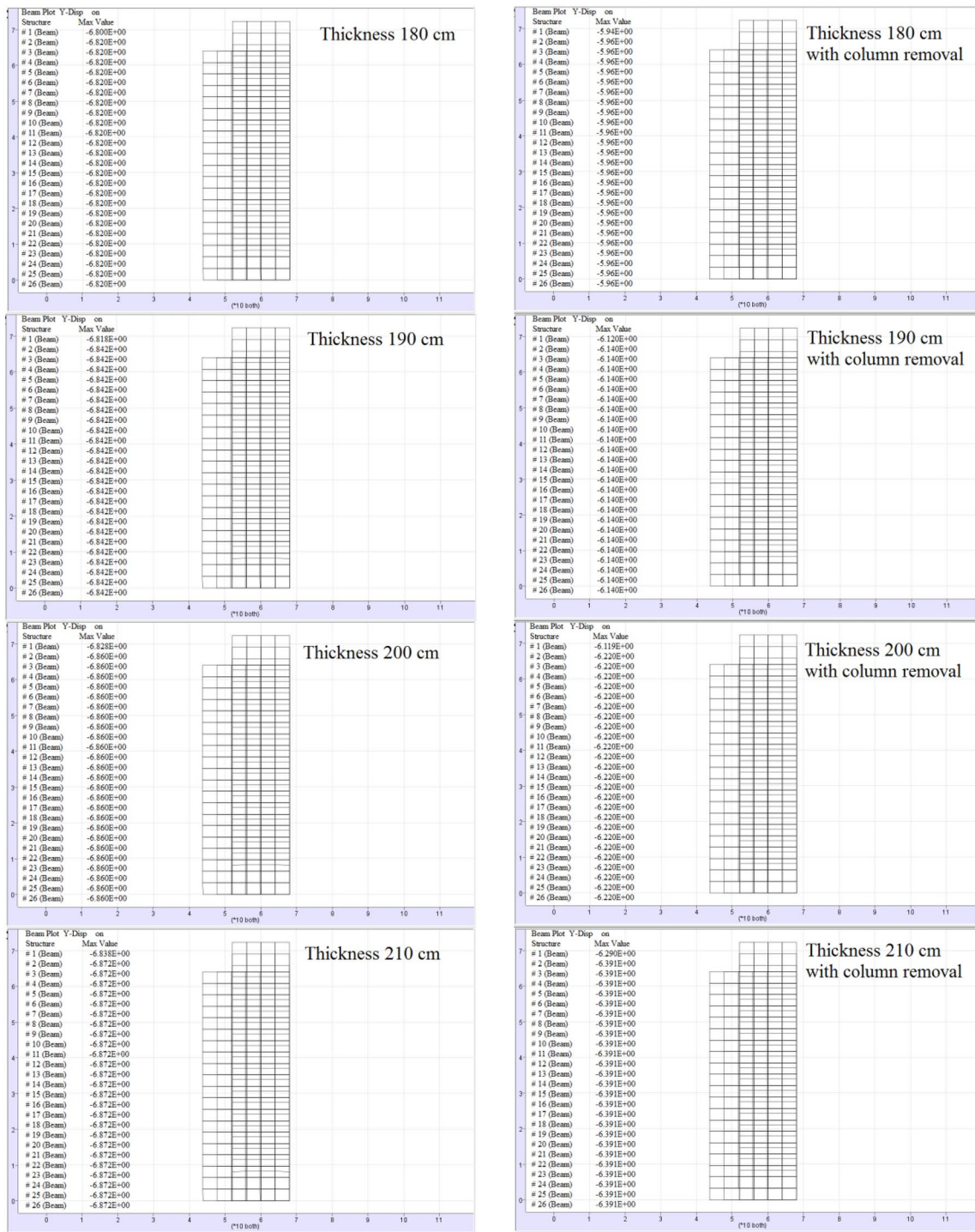
$$(11)$$

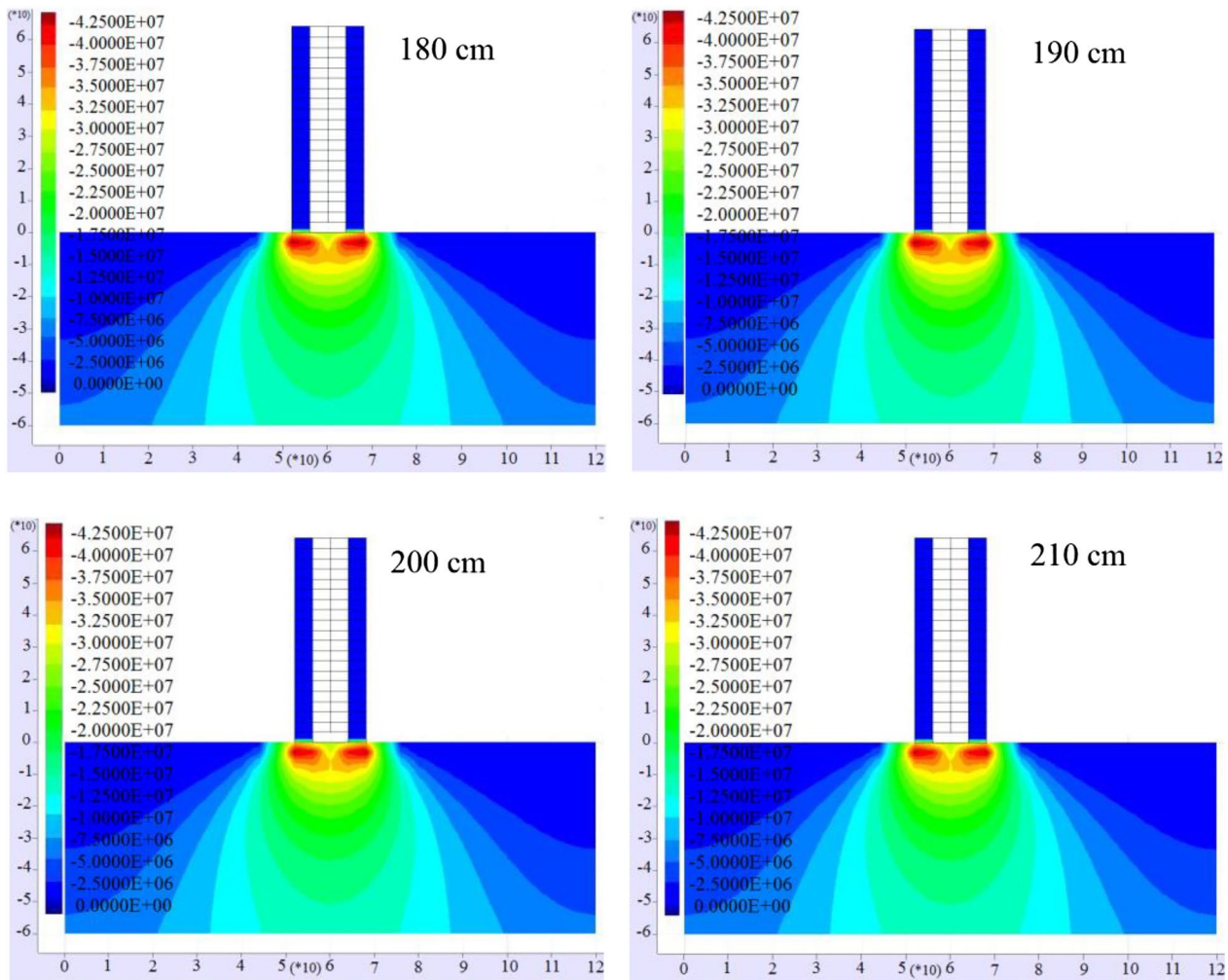**Fig. 8** Displacements of the frames with different thicknesses of foundation

Fig. 9 SYY contours of RCSWs frames following the middle column removal with various thicknesses of foundation
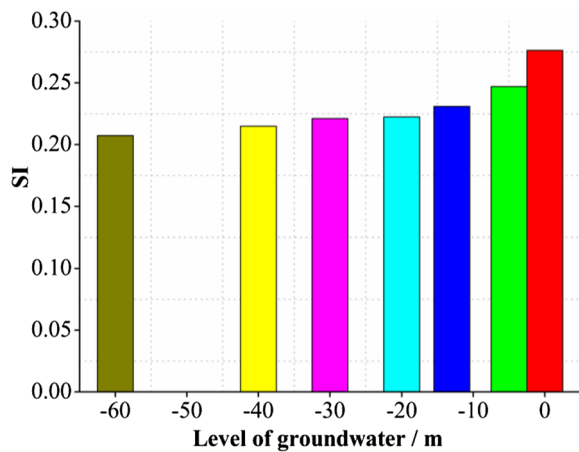

Fig. 10 Plot of the sensitivity index versus different levels of groundwater in the substructure soil

Table 5 Redistribution of the imposed loads in the 20-story RCSWs frames with various groundwater levels in the substructure soil

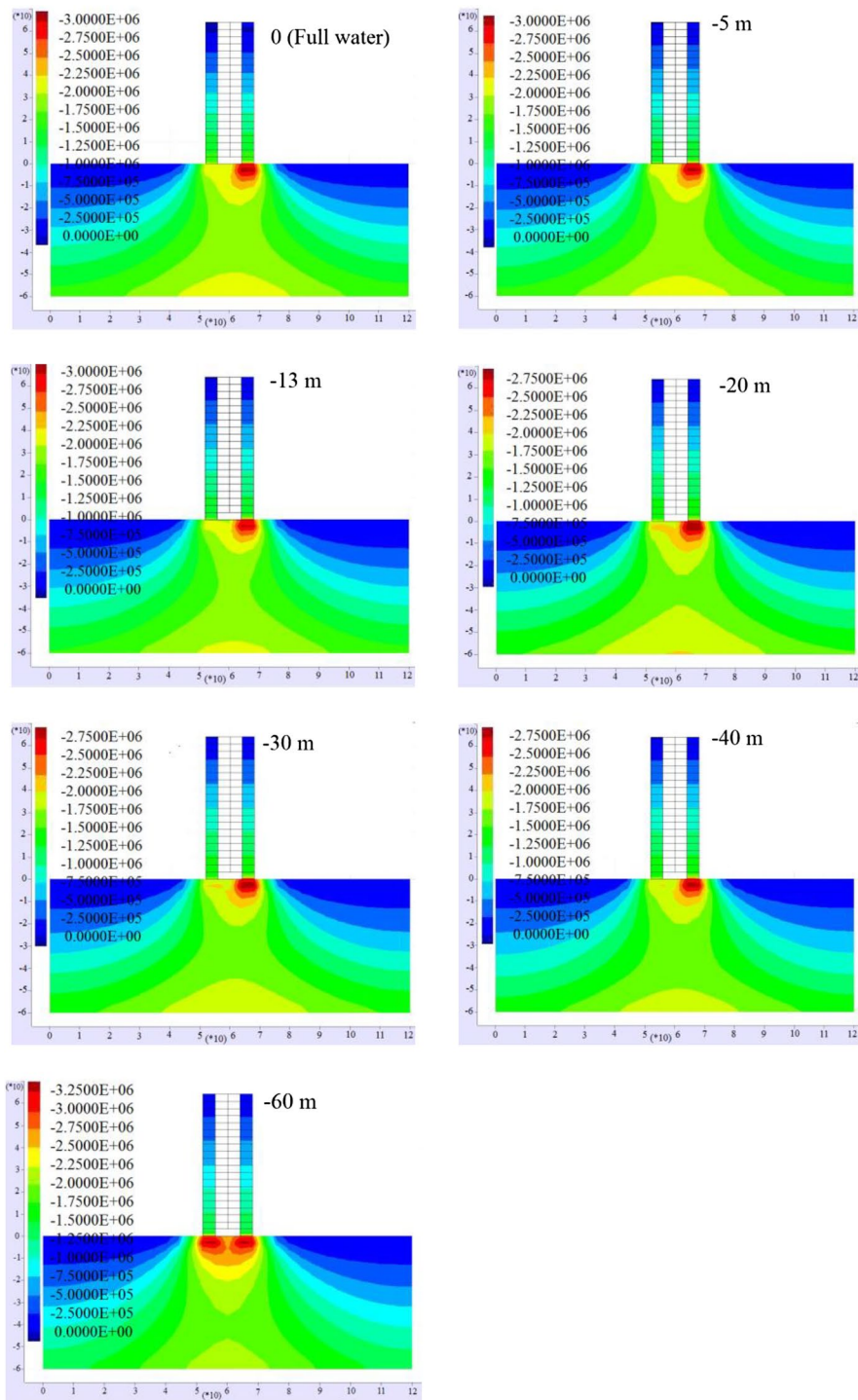| levels of groundwater (m)	λ_0 (kN)	λ_{damage} (kN)	SI
0 (Full water)	6218	4499.8	0.2763
− 5	5964	4490.9	0.2470
− 13	5828	4482.5	0.2309
− 20	5636	4382.3	0.2224
− 30	5462	4254.1	0.2211
− 40	5343.4	4194.7	0.2149
− 60	5162	4092	0.2073

Fig. 11 SYY contours of RCSWs frames after removing the middle column with various levels of groundwater

Table 6 Characteristics of the various types of the substructure soil (Qian et al., 2022)

Soil type	Dry density (kg/m³)	Bulk modulus (MPa)	Shear modulus (MPa)	Friction angle (degree)	Cohesion (Pa)	Dilation angle (degree)	Tensile strength (Pa)
Rock	2700	555.50003	416.6	33	10,000	0.0	1000
SM	1980	30.30	25.60	32	0.0	0.0	0.0
CL–ML	1880	16.670001	10.17	30	0.0	0.0	0.0
GW	1700	78.43	53.20	38	0.0	0.0	0.0
Clay–MC	1600	11.1111	3.703700	25	5000	0.0	0.0

k is the coefficient that accounts for the effects of the proposed model on bond stress, and f_R is the relative rib area. From the position of the reinforcing bar during casting and depending on whether or not a stirrup is used, k can be classified as follows:

$$k = 0.2 \times \exp\left\{ \left[-4.5 + 55(3.06f_R - 0.24)\right] \times \frac{100}{A_c} \right\}$$

(Vertically cast bar),

$$k = 0.2 \times k_{sh} \times \exp\left\{ \left[-4.5 + 55(3.06f_R - 0.24)\right] \times \frac{100}{A_c} \right\}$$

(Vertically cast bar with stirrups),

$$k = 0.2 \times \exp\left\{ \left[-4.5 + 55f_R\right] \times \frac{100}{A_c} \right\} \quad \text{(Horizontally cast bar),}$$

$$k = 0.2 \times k_{sh} \times \exp\left\{ \left[-4.5 + 55f_R\right] \times \frac{100}{A_c} \right\} \tag{12}$$

(Horizontally cast bar with stirrups)

A_c is the cross-sectional area of the concrete. k_{sh} is the coefficient which express the stirrups' effect (1.0 for a vertically cast stirrup, 0.85 for a horizontally cast stirrup), and f_R is the relative rib area.

The reciprocal value of the cross-sectional area of concrete ($100/A_c$) has the same meaning as the average stress of the corresponding cross-sectional area of concrete falling under the unit load. In this study, it is believed that the size effects of the cross section need to be considered in accordance with the cross-sectional area of concrete, which is actually loaded.

After modeling the 20-story RCSWs frames in SeismoStruct software, the frames and the substructure soil (hard soil) were modeled in FLAC software and verified. The total base shears of RCSWs frames with and without the middle column removal are represented in Fig. 5. The results of the numerical models in SeismoStruct and FLAC softwares are shown in Table 3. As shown, there is

a good agreement between the mentioned models. The sensitivity index values of the 20-story RCSWs frames in SeismoStruct and FLAC softwares and RC frames in FLAC software are shown in Fig. 6. As shown, the SI value of the RCSWs frame in FLAC software is less than the RCSWs frame in SeismoStruct software. It means that the sensitivity index value decreases by considering the SSI. Shear forces and flexural anchors in RCSWs frames are reduced by simultaneous modeling of soil (hard soil), foundation and RCSWs frames in FLAC software. This causes the use of smaller dimensions for the design of structural elements.

Also, in this research, the effect of shear wall was investigated in the progressive collapse of the 20-story RCSWs frames. For this purpose, the vulnerability of RC and RCSWs frames was investigated following the column removal from the first story. The sensitivity indexes of the 20-story RCSWs and RC frames by considering the SSI are shown in Fig. 6. It was demonstrated that the use of the reinforced concrete shear walls decreases the sensitivity index by 5.25%. As a result, the conditions are improved to prevent progressive collapse.

In the flexural wall-frames (RCSWs frames), the flexural frame and the shear wall together resist lateral forces. In fact, the shear wall and flexural frame are each deformed in bending and shear modes, respectively. In the lower stories, the behaviour of the shear wall is more effective and in the upper stories, the flexural frames' behavior is more effective. The interaction between the flexural frame and shear wall is proportion to the structural stiffness. As the stiffness of the flexural frame increases, the amount of interaction increases. The main advantages of considering the flexural frame-shear wall interaction in the design of the RCSWs frames can be mentioned below. In flexural wall-frames, the displacement and flexural anchors are less than RC frames. In the flexural wall-frames, the shear in supports is more uniform and economical, and they have more ductility, indeterminacy and safety than RC frames (Stafford Smith & Coull, 1991).
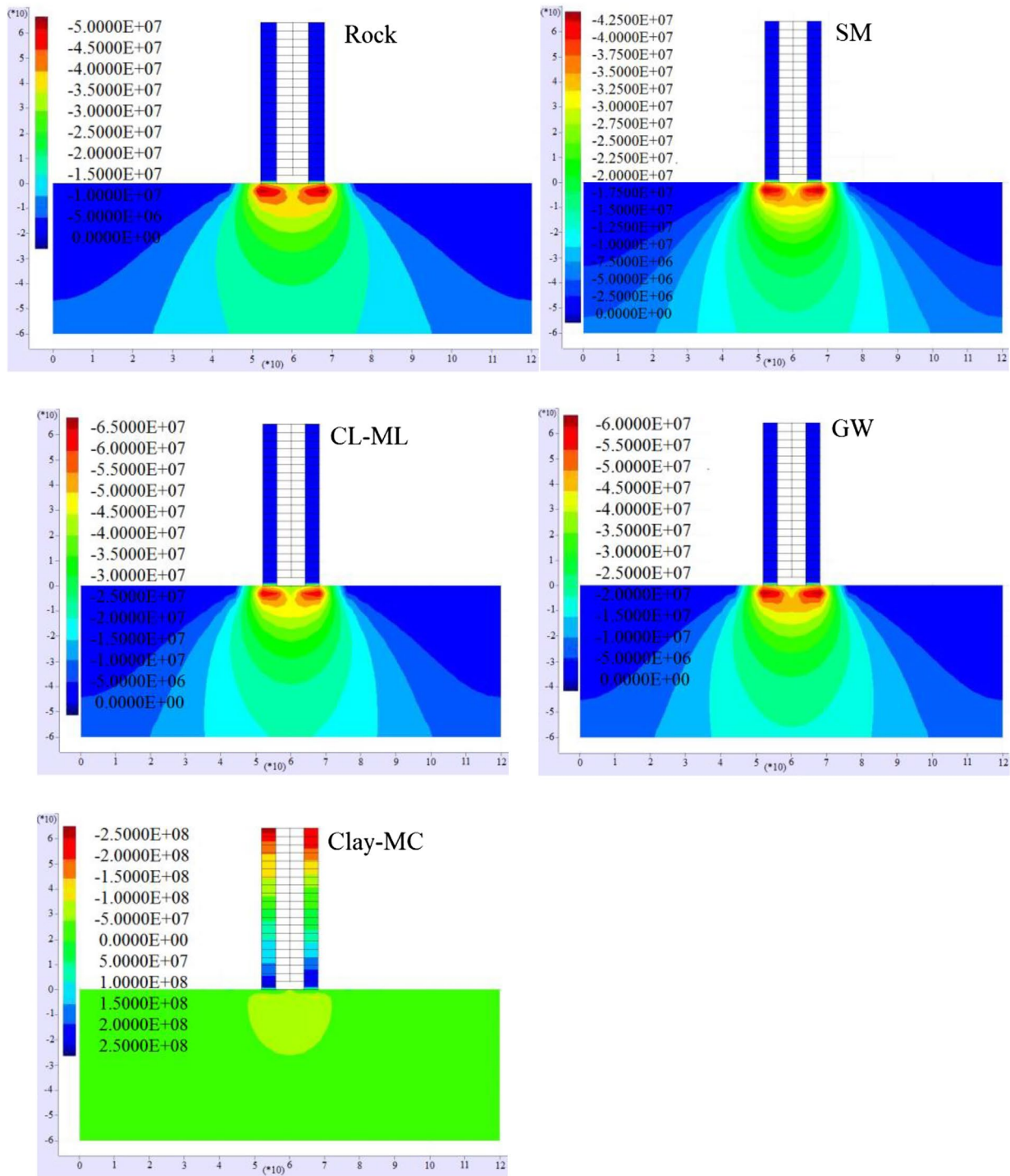
Fig. 12 SYY contours of the RCSWs frames following the column removal with various soil types

Table 8 Redistribution of the imposed loads in the 20-story RCSWs frames with different soil densities

Soil density (kg/m³)	λ_0 (kN)	λ_{damage} (kN)	SI
1600	5219.2	4126.4	0.2094
1800	5147.8	4162.8	0.1913
2000	5025.8	4196.8	0.1649
2200	5016.4	4225.2	0.1577

4 Parametric Analyses

As the RCSWs frames were modeled in FLAC software, the effects of various parameters, including the thickness of foundation, soil saturation condition, soil type, soil density, and the substructure soil layers, were assessed on the progressive collapse of RCSWs frames.

4.1 Thickness of Foundation

The effect of the thickness of foundation on the progressive collapse of RCSWs frames was investigated following the middle column removal. For this purpose, a 20-story RCSWs frame with different foundation thicknesses of 180, 190, 200, and 210 cm, along with the substructure, was modeled in FLAC software with and without removing the middle column. The vulnerability of the frames to progressive collapse was determined based on the sensitivity index. Loading was performed in the structures according to the DoD guidelines. The values of λ_0 and λ_{damage} and the obtained sensitivity index are represented for each thickness of the foundation in Table 4. As shown in Table 4 and Fig. 7, as the foundation thickness decreases from 210 to 180 cm, the sensitivity index decreases by 5.9%. Therefore, RCSWs frames with a foundation thickness of 180 cm have better conditions in preventing progressive collapse.
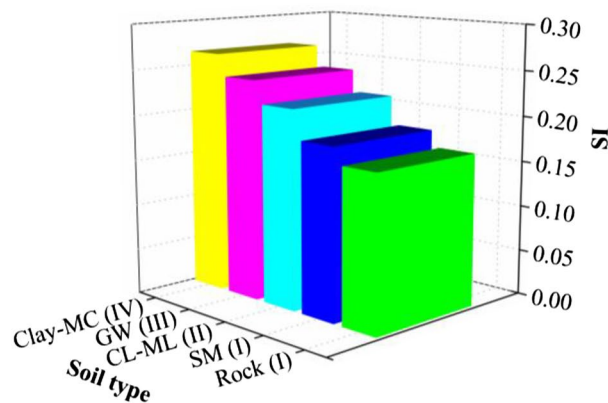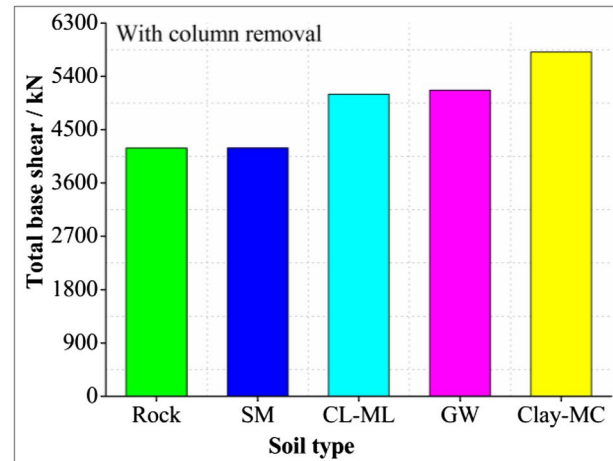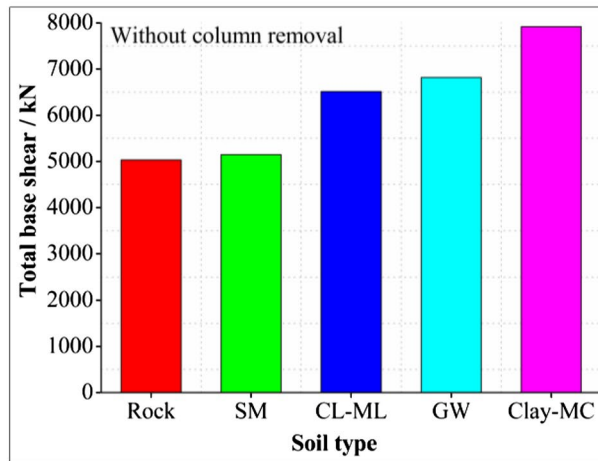

Fig. 13 Total base shear with and without column removal and the plot of the sensitivity index for different substructure soil types

Table 7 Redistribution of the imposed loads in the 20-story RCSWs frames with various types of the substructure soil

Soil type	λ_0 (kN)	λ_{damage} (kN)	SI
Rock	5032.6	4189.4	0.1675
SM	5147.8	4191.8	0.1857
CL–ML	6514	5098	0.2174
GW	6818	5166.6	0.2422
Clay–MC	7919	5811.3	0.2662
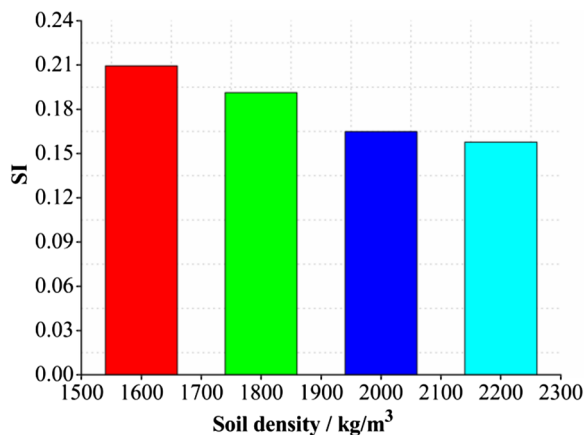
Fig. 14 Plot of the sensitivity index versus the substructure soil density

Foundations of the structures are under the influence of the flexural anchorage in addition to the axial load. Flexural anchorage in a structural member occurs when the moment, applied to the member, causes bending. Anchor is known as the product of force by distance. The tensile and compressive stresses of the structural members change in proportion to the change in the size of the bending moment. In fact, in a flexural wall-frame, despite the fact that the bending and flexural anchors in the support are less than a simple frame with a shear wall, still in this case, the vertical stress distribution on the soil is not uniform and the bearing capacity of the soil decreases, because in this case, the length with the effective width of the foundation or both of them will be less than the actual value. To calculate the effective length and width of the foundations, it is assumed that the load enters the geometric center of the equivalent foundation and the parts of the foundation that are outside this range are ignored.

In fact, as the thickness of the foundation and consequently its weight increases, the anchor's amount increases. With an increase in the foundation thickness, the average subsidence, maximum subsidence and flexural anchorage of the foundation increase. The only

positive influence of increasing the thickness of the foundation is reducing its non-uniform subsidence.

The displacements of the frames with different foundation thicknesses are shown in Fig. 8. The results demonstrated that with the increase in the foundation thickness, the displacement increased. SYY is the force per unit area acting in the *Y* direction on a plane perpendicular to the *Y* axis. The changes in SYY contours of the RCSWs frames with different foundation thicknesses following the middle column removal are represented in Fig. 9. SYY contours are utilized to show the redistribution of force after removing the column and the stress changes in the substructure of the adjacent columns of the removed one.

4.2 Soil Saturation Condition

The influence of the soil saturation conditions on the progressive collapse of RCSWs frames was evaluated by considering different groundwater levels for the substructure soil. For this purpose, the 20-story RCSWs frames with and without the middle column removal were modeled in FLAC software. SM–CL/ML (Very hard clay)–SM was utilized as the substructure soil layer.

Loading in the frames was performed according to the DoD regulations, and the sensitivity index was obtained for each level of groundwater (Fig. 10). As shown in Fig. 10 and Table 5, by decreasing the groundwater level of the substructure soil from 0 (Full water) to −60 m (dry), the sensitivity index decreases by 25%. Thus, the conditions of the frames are improved to prevent progressive collapse.

The SYY contours of the RCSWs frames following the middle column removal with various levels of groundwater are represented in Fig. 11. As can be seen, after removing the middle column, redistribution of force takes place and the stress in the substructure of the columns adjacent to the removed one increase.

Actually, with the rise of the groundwater level, the water content of the soil gradually increases, and the soil changes from an unsaturated state to a saturated state. The rise of the groundwater in the fine-grained soils causes the swelling of the soil grains and in the coarse-grained soils it causes the reduction of the internal friction angle of soil grains.

In case of saturation of the soil layer, the movement of soil particles and, finally the sudden subsidence occur due to the change of the stress amplitude. This is due to the effect of soil saturation conditions on the reduction of the resistance parameters, such as shear strength, shear modulus, friction angle and subsequently, the sudden subsidence of the soil.

As a result of the above mentioned parameters, with the increase in the groundwater level, the condition of
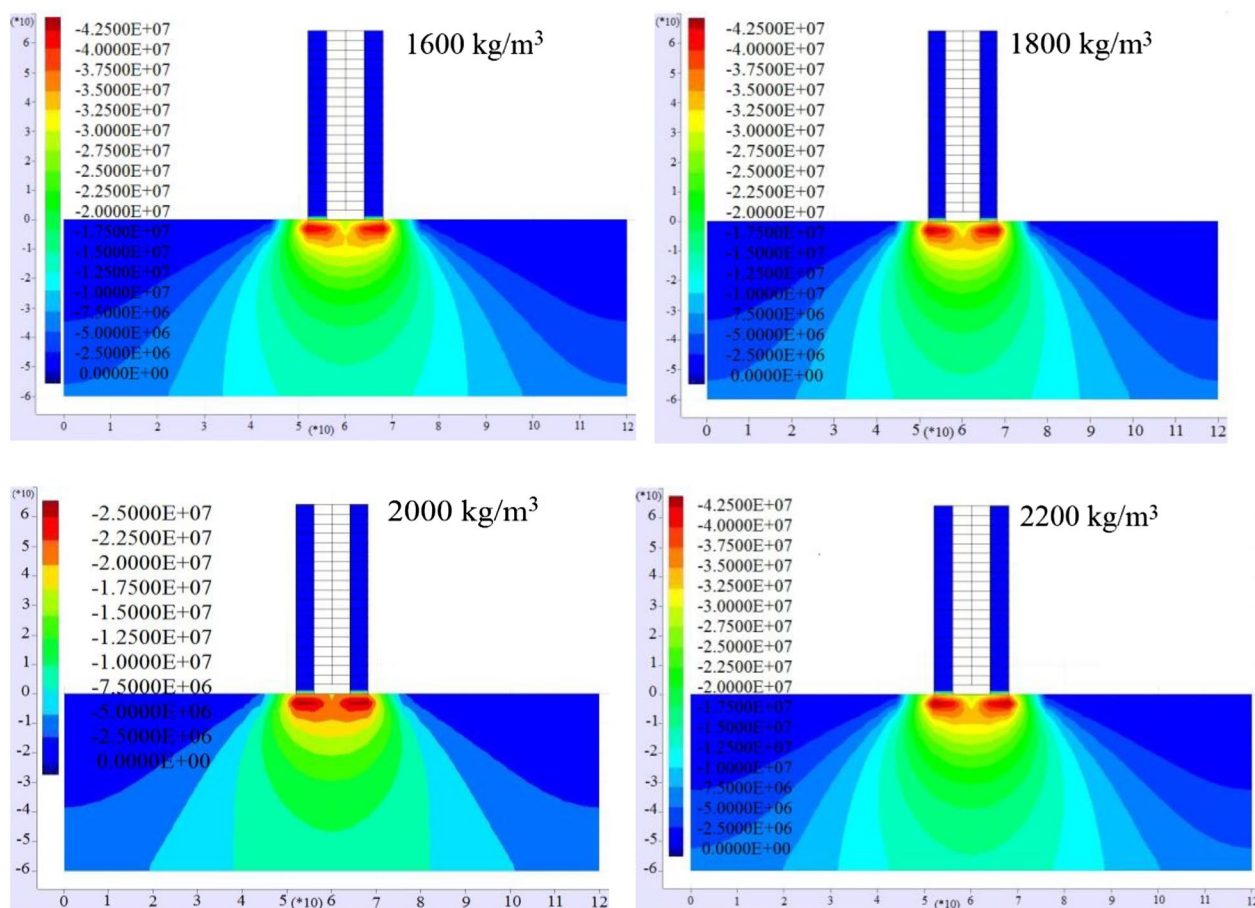
Fig. 15 SYY contours of the RCSWs frames following the column removal with various soil densities

the substructure soil is out of the previous stable state (unsaturated soil) and leads to the uneven stress in the soil. This mechanism can be seen by comparing the SYY contours of the RCSWs frames in the saturate states (0, −13, −20, −30, and −40 m) with the dry state (−60 m). In the dry state, the stress distribution is symmetric and in the saturate states, it is asymmetric.

This result is also consistent with the experimental research conducted by Chen et al. (2022). The experimental research showed that as the groundwater level increases, the compressive index increases. While the compressive modulus, cohesion, and internal friction angle gradually decrease, the soil gradually softens, and the shear strength decreases, which leads to a decrease in the bearing capacity of the foundation and an increase in the foundation deformation. This leads to the destruction of the foundation and damage to the structure. Therefore, it is better to drain the soil before building the structure in areas with high groundwater levels.

4.3 Soil Type

The influence of various soil types on the progressive collapse of RCSWs frames was evaluated following the middle column removal. For this purpose, the 20-story RCSWs frames with different soil types of Rock, silty sands (SM), well-graded gravel (GW), clay–clayey silt (Clay-MC), and silty clay with low plasticity (CL–ML) for substructure were modeled in FLAC software with and without removing the middle column. The characteristics of the studied substructure soils are represented in Table 6 (Qian et al., 2022). Loading was performed in the frames according to the DoD guidelines. It is observed that the soil type is very effective in investigating the effects of soil–structure interaction. In fact, the dynamic effects of soil–structure interaction depend on various factors, such as the geometry characteristics, stiffness, mass and damping of the structure, and substructure soil type. Therefore, to investigate the effect of soil type on the progressive collapse of the frames, the characteristics
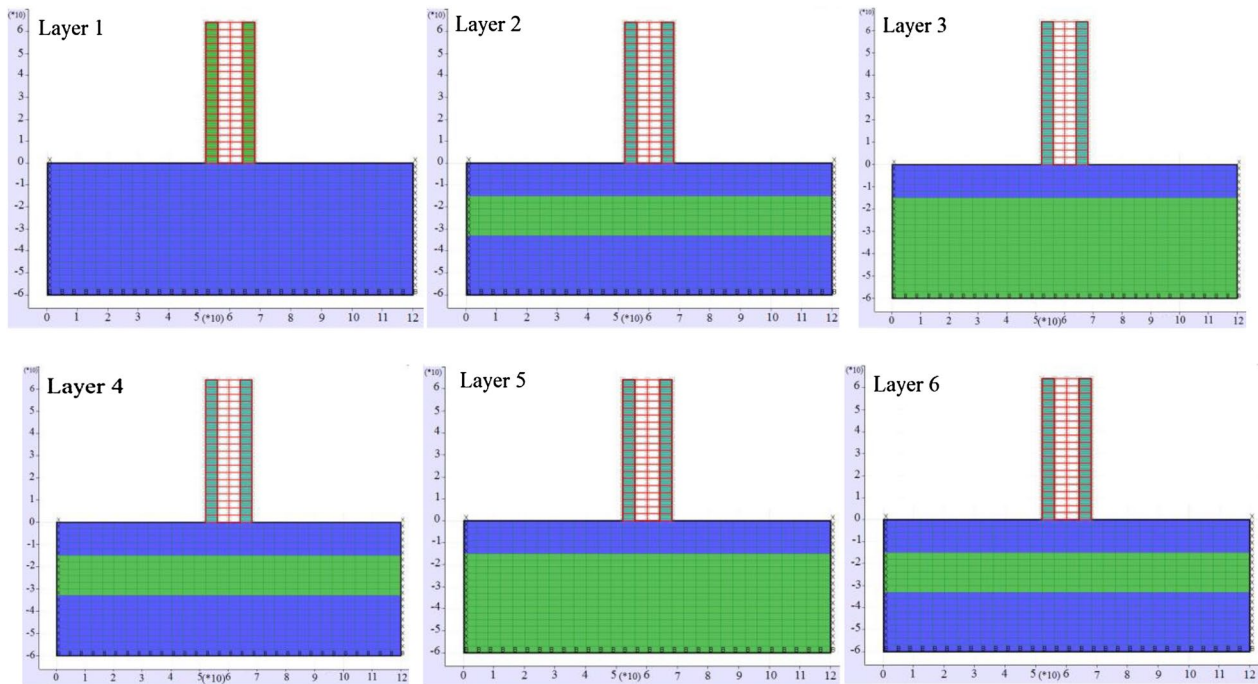
Fig. 16 Modeling of the 20-story RCSWs frames with various soil layers in FLAC software

Table 9 Characteristics of the different substructure soil layers (Qian et al., 2022)

Soil type	Dry density (kg/m³)	Bulk modulus (MPa)	Shear modulus (MPa)	Friction angle (degree)	Dilation angle (degree)	Cohesion (Pa)	Tensile strength (Pa)
SM	1980	30.30	25.60	32	0.0	0.0	0.0
CL–ML (very hard clay)	1910	33.330002	20.25	30	0.0	0.0	0.0
CL–ML (hard clay)	1880	16.670001	10.17	30	0.0	0.0	0.0
Very soft clay	582	1.6699999	0.172	0.0	0.0	5000	0.0

Table 10 Cross-sectional features of the substructure soil layers

Depth (m)	0–10	10–15	15–60
Layer 1	SM	SM	SM
Layer 2	SM	CL/ML (Very hard clay)	SM
Layer 3	SM	CL/ML (Very hard clay)	CL/ML (Very hard clay)
Layer 4	SM	CL/ML (Hard clay)	SM
Layer 5	SM	CL/ML (Hard clay)	CL/ML (Hard clay)
Layer 6	SM	Very soft clay	SM

of geometry, stiffness, mass and damping of the structures were considered the same and only different soil types were investigated.

The SYY contours of the RCSWs frames after column removal with various substructure soil types are represented in Fig. 12. It can be seen that after removing a column, redistribution of force takes place and the stress in the substructure of the columns adjacent to the removed column increases. As shown in the SYY contours of the RCSWs frames with different soil types, by changing the soil type from rock (hard soil) to Clay-MC (soft soil), the stress increases. This happens because of the specific properties of the soft soils, including the large void ratio, high compressibility, low permeability, and low shear strength. The flexibility of the substructure soil increases the displacement of the stories, base shear and time period of the structure.

The values of λ_0 and λ_{damage} and the obtained sensitivity indexes for the frames with different substructure soil types are exhibited in Table 7. As the substructure soil types change from Rock to Clay-MC, the sensitivity

Table 11 Redistribution of imposed loads in the RCSWs frames with various soil layers

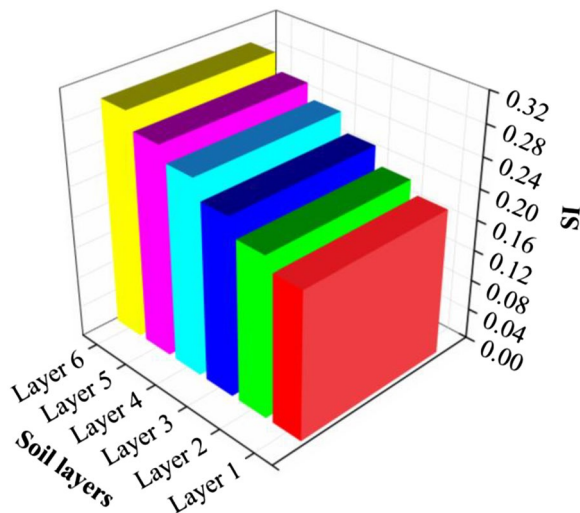| Layers	Soil layers	λ_0 (kN)	λ_{damage} (kN)	SI
Layer 1	SM	5147.8	4162.8	0.1913
Layer 2	SM–CL/ML (Very hard clay)–SM	5162	4092	0.2073
Layer 3	SM–CL/ML (Very hard clay)–CL/ML (very hard clay)	5368.4	4133	0.2301
Layer 4	SM–CL/ML (Hard clay)–SM	6084	4540.4	0.2540
Layer 5	SM–CL/ML (Hard clay)–CL/ML (Hard clay)	6414	4665.8	0.2725
Layer 6	SM–Very soft clay-SM	8188	5780	0.2941

Fig. 17 Plot of sensitivity index versus soil layers

index increases by 59% (Fig. 13). Thus, compared to other soil types, Rock and SM are better for preventing progressive collapse.

4.4 Soil Density

The effect of soil density was investigated on the progressive collapse of RCSWs frames following the middle column removal. For this purpose, different soil densities of 1600, 1800, 2000 and 2200 kg/m^3 were examined. The frames with different densities of the substructure soil with and without column removal were modeled in FLAC software. Loading in the frames was done according to the DoD regulations, and the sensitivity indexes were obtained (Fig. 14). As shown in Fig. 14 and Table 8, the sensitivity index decreased by 24.7% by increasing the density of the substructure soil from 1600 kg/m^3 to 2200 kg/m^3. As a result, the condition of the RCSWs frames will be better to prevent progressive collapse. Thus, the density of the substructure soil can be increased by deliberate compaction. With an increase in the soil density, the pore spaces in the soil structures

and drainage channels between the soil structures are removed. This prevents the penetration of plant roots into the soil and prevents the movement of air and water in it. Soil compaction can be done in two ways, intentional or unintentional, among which intentional soil compaction is desirable.

Various methods are used for soil compaction, including vibration compaction, dynamic compaction, explosion in soil compaction, etc. The exit of water and air from the soil mass with compaction causes a decrease in porosity, an increase in specific weight, and as a result, an increase in the relative density of the soil. Increasing the relative density of the soil has many advantages, including improving soil properties, increasing soil resistance properties, bearing capacity of the soil, bearing capacity of surface and deep foundations, and reducing the inappropriate soil subsidence and risk of liquefaction. From the behavioral point of view, the increase in the relative density of the soil, in addition to the increase in the specific weight of the soil, causes an increase in the properties, such as the shear modulus, bulk modulus, elasticity modulus, standard penetration coefficient and internal friction angle of the soil. In fact, the presence of hard and dense soil with high relative density provides ideal conditions for geotechnical designs.

SYY contours of the RCSWs frames with different soil densities following the middle column removal are represented in Fig. 15. As shown, after removing the column, the stress in the substructure of the columns adjacent to the removed column increases and forces are redistributed.

4.5 Substructure Soil Layers

The term soil layer refers to a soil horizon that runs parallel to the soil surface. Each layer of soil has unique biological and chemical characteristics from the preceding or subsequent layer. Soil layers are deposits that have formed over a long time. Soil layers gain strength and stability with time. Water, wind, glaciers, and human activity all have a hand in the formation of soil layers.
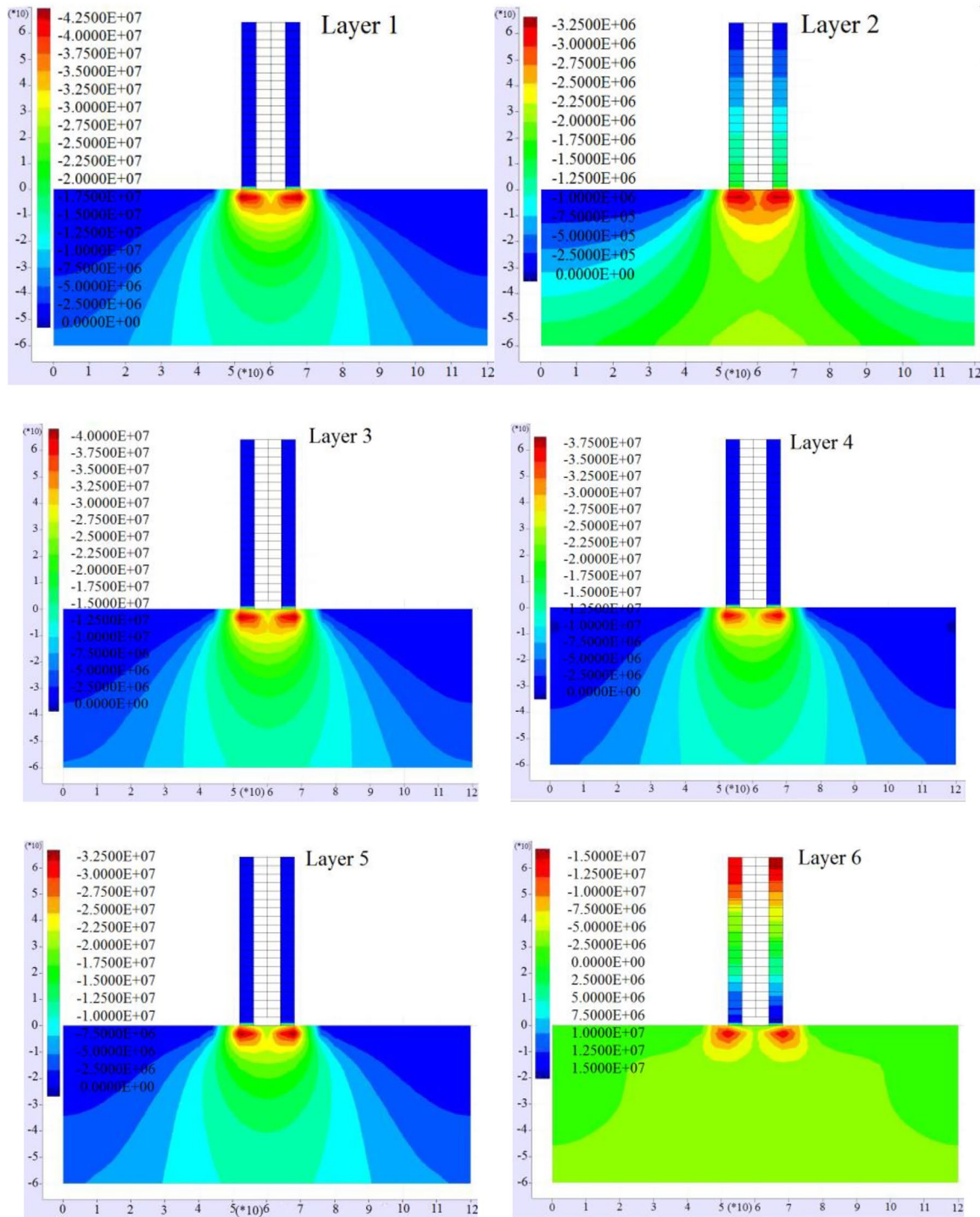
Fig. 18 SYY contours of the RCSWs frames following the column removal with different soil layers

In the investigation of different types of substructure soil, it was found that SM has good conditions against progressive collapse. Thus, in evaluating the effect of different substructure soil layers on the progressive collapse of the RCSWs frames, SM was utilized as one of the main components of all layers. To investigate the effect of various substructure soil layers on the progressive collapse of the RCSWs frames, a 20-story RCSWs frame with

different soil layers of SM (layer 1), SM–CL/ML (Very hard clay)–SM (layer 2), SM–CL/ML (Very hard clay)–CL/ML (very hard clay) (layer 3), SM–CL/ML (Hard clay)–SM (layer 4), SM–CL/ML (Hard clay)–CL/ML (Hard clay) (layer 5), and SM–Very soft clay–SM (layer 6) were modeled in FLAC software and subjected to the column removal scenario. Modeling of the RCSWs frames without removing the middle column with various soil layers is represented in Fig. 16. The characteristics of the different soil layers are mentioned in Table 9. The cross-sectional features of the soil layers are shown in Table 10. Loading was done in the RCSWs frames according to the DoD guidelines. The sensitivity index values were calculated for each soil layer (Table 11). As shown in Fig. 17, by changing the soil layer from layer 1 (SM) to layer 6 (SM–Very soft clay–SM), the sensitivity index increases by 53.7%. The type of soil layering affects the displacement of the frames. In fact, the displacement increased with the change of soil layer from layer 1 (SM) to layer 6 (SM–very soft clay–SM).

Therefore, layers 1 and 2 are better than other soil layers in preventing progressive collapse. The SYY contours of the RCSWs frames following the middle column removal with different soil layers are represented in Fig. 18. As shown, after removing the column, redistribution of the force takes place and the stress in the substructure of the columns adjacent to the removed column increases.

5 Conclusions

In this research, progressive collapse of the 20-story RCSWs frames was investigated with and without considering the soil–structure interaction in the FLAC and Seismostruct softwares, respectively. Afterward, a parametric study including thickness of foundation, soil density, soil type, soil saturation conditions, and different soil layers was performed. The vulnerability of the RCSWs frames against progressive collapse was determined following the middle column removal from the first story and using the sensitivity index. The obtained results are as follows:

– By comparing the modeling results of the 20-story RCSWs frames in SeismoStruct and the simultaneous modeling of soil (hard soil), foundation and RCSWs frame in the FLAC software, it can be seen that considering the effect of soil–structure interaction leads to a decrease in the sensitivity index. Actually, by taking into account the effect of SSI, the shear forces and flexural anchors in the RCSWs frames are reduced, making it possible to use smaller dimensions for designing the structural elements.

– The results showed that with the increase in the thickness of the foundation from 180 to 210 cm, the sensitivity index increased by 6.3%. Furthermore, the results showed that the displacement of the stories increased with the increase in the foundation thickness. Therefore, the foundation thickness of 180 cm with less displacement and lower sensitivity index has better conditions against progressive collapse. In fact, as the thickness of the foundation increases, the maximum subsidence, average subsidence and flexural anchorage of the foundation increase. Its only positive effect can be the reduction of non-uniform foundation subsidence.

– It was shown that by increasing the soil density from 1600 to 2200 kg/m^3, the sensitivity index decreases by 24.7%. As a result, by increasing the soil density, the conditions for preventing progressive collapse are improved.

– The results demonstrated that by changing the substructure soil type from type 1 (Rock) to type 4 (Clay–MC), the sensitivity index increased by 59%. As a result, in the 20-story RCSWs frame, by changing the type of substructure soil from type 4 to type 1, the conditions are improved to prevent progressive collapse.

– It was found that by changing the substructure soil layer from layer 1 to layer 6, the sensitivity index increased by 53.7%. As a result, among different studied soil layers, layer 1 (SM) and layer 2 (SM–CL/ML (Very hard clay)–SM) are better to prevent progressive collapse.

– It was found that by lowering the groundwater level from 0 (full water) to −60 m (dry), the sensitivity index decreased by 25%, and the condition would be better to prevent the progressive collapse. High groundwater levels in the subsoil can reduce its bearing capacity and lead to the destruction of the foundation and damage to the structure. Consequently, the dry condition of the substructure soil is ideal for preventing progressive collapse. Therefore, in areas with high groundwater levels, it is better to drain the soil before building the structure.

Ekrami Kakhki *et al. Int J Concr Struct Mater*   (2023) 17:22

Page 22 of 24

Authors' Information
Seyed Ali Ekrami Kakhki is a Ph.D. student of Structural Engineering, Civil Engineering Department, Semnan Branch, Islamic Azad University, Semnan, Iran. His research interests include the progressive collapse of concrete structures, tall buildings, and soil–structure interaction.
Ali Kheyroddin is a Distinguished Professor, Department of Civil Engineering, Semnan University, Semnan, Iran. His research interests include design of reinforced concrete structures, tall buildings, rehabilitation of buildings, progressive collapse of structures, and design of earthquake resistant buildings.
Alireza Mortezaei is an Associate Professor, Seismic Geotechnical and High Performance Concrete Research Centre, Civil Engineering Department, Semnan Branch, Islamic Azad University, Semnan, Iran. His research interests include RC structures, soil–structure interaction, and reliability of structures.

Availability of data and materials
Not applicable.

Declarations

Ethics approval and consent to participate
Not applicable.

Consent for publication
Not applicable.

Competing interests
The authors declare that they have no conflict of interest.

References
Adam, J. M., Parisi, F., Sagaseta, J., & Lu, X. (2018). Research and practice on progressive collapse and robustness of building structures in the 21st century. *Engineering Structures, 173*, 122–149. https://doi.org/10.1016/j.engstruct.2018.06.082

Al-Ghalibi, F. Y., & Al-Hadithy, L. (2018). RC walls under seismic effects, general review. *International Journal of Civil Engineering and Technology (IJCIET), 9*, 888–916.

Alshaikh, I. M. H., Abu Bakar, B. H., Alwesabi, E. A. H., & Akil, H. M. (2020). Experimental investigation of the progressive collapse of reinforced concrete structures: An overview. *Structures, 25*, 881–900. https://doi.org/10.1016/j.istruc.2020.03.018

Anvarsamarin, A., Rahimzadeh Rofooei, F., & Nekooei, M. (2020). Torsion effect on the RC structures using fragility curves considering with soil-structure interaction. *Journal of Rehabilitation in Civil Engineering, 8*, 1–21. https://doi.org/10.22075/jrce.2019.16080.1302

Azimi, M., & Molaei Yeznabad, A. (2020). Swarm-based parallel control of adjacent irregular buildings considering soil–structure interaction. *Journal of Sensor and Actuator Networks, 9*, 1–24. https://doi.org/10.3390/jsan9020018

Bao, Y., & Kunnath, S. K. (2010). Simplified progressive collapse simulation of RC frame-wall structures. *Engineering Structures, 32*, 3153–3162. https://doi.org/10.1016/j.engstruct.2010.06.003

Behnamfar, F., & Banizadeh, M. (2016). Effects of soil–structure interaction on distribution of seismic vulnerability in RC structures. *Soil Dynamics and Earthquake Engineering, 80*, 73–86. https://doi.org/10.1016/j.soildyn.2015.10.007

Cavalieri, F., Correia, A. A., Crowley, H., & Pinho, R. (2020). Dynamic soil-structure interaction models for fragility characterisation of buildings with shallow foundations. *Soil Dynamics and Earthquake Engineering, 132*, 106004. https://doi.org/10.1016/j.soildyn.2019.106004

Chehab, A. I., Eamon, C., & Griffin, J. (2017). Collapse resistance of RC moment-resisting frame and shear wall structural systems exposed to blast. *Journal of Performance of Constructed Facilities, 31*, 1–39. https://doi.org/10.1061/(ASCE)CF.1943-5509.0000957

Chen, W., Liu, Q., & Wang, E. (2022). The effect of the water table on the bearing capacity of a shallow foundation. *Applied Sciences, 12*, 6571. https://doi.org/10.3390/app12136571

Department of Defense (DoD). (2013). *Unified facilities criteria (UFC 4–010-01), DoD minimum antiterrorism standards for buildings*. Department of Defense.

Department of Defense (DoD). (2016). *Unified facilities criteria (UFC 4–023-03), design of buildings to resist progressive collapse, with change 3*. Department of Defense.

Elmagbool, M. M. G., Muniraj, K., Parthiban, P., & Mostafa, O. (2021). Study the progressive collapse analysis of shear wall-framed building for different soil profile types S_C, S_D. *Journal of Building Pathology and Rehabilitation, 6*, 1–8. https://doi.org/10.1007/s41024-021-00109-2

Elsanadedy, H. M., & Abadel, A. A. (2022). High-fidelity FE models for assessing progressive collapse robustness of RC ordinary moment frame (OMF) buildings. *Engineering Failure Analysis, 136*, 106228. https://doi.org/10.1016/j.engfailanal.2022.106228

Esmaeilnia Omran, M., & Hoseini Karani, A. (2018). Span length effects on the progressive collapse behaviour in concrete structures. *Journal of Stress Analysis, 3*, 81–91. https://doi.org/10.22084/jrstan.2018.16441.1050

European Committee for Standardization. (2004a). *EN 1992-1-1:2004, Eurocode 2: Design of concrete structures – Part 1–1: General rules and rules for buildings*. European Committee for Standardization.

European Committee for Standardization. (2004b). *EN 1998–1–5:2004, Eurocode 8: Design of structures for earthquake resistance – Part 1–5: Specific rules for concrete buildings*. European Committee for Standardization.

Faghihmaleki, H. (2017). Assessment of robustness index and progressive collapse in the RC frame with shear wall structure under blast loading. *Journal of Applied Research on Industrial Engineering, 4*, 59–66. https://doi.org/10.22105/jarie.2017.49601

Far, H. (2019). Advanced computation methods for soil-structure interaction analysis of structures resting on soft soils. *International Journal of Geotechnical Engineering, 13*, 352–359. https://doi.org/10.1080/19386362.2017.1354510

Far, H., & Flint, D. (2017). Significance of using isolated footing technique for residential construction on expansive soils. *Frontiers of Structural and Civil Engineering, 11*, 123–129. https://doi.org/10.1007/s11709-016-0372-8

Farahani, A., Kheyroddin, A., & Sharbatdar, M. K. (2018). Finding critical element in the progressive collapse of RC structures using sensitivity analysis. *Civil Engineering Journal, 4*, 3038–3057. https://doi.org/10.28991/cej-03091219

Fathi, A., Sadeghi, A., Emami Azadi, M. R., & Hoveidaie, N. (2020). Assessing seismic behavior of a masonry historic building considering soil-foundation-structure interaction (Case study of Arge-Tabriz). *International Journal of Architectural Heritage, 14*, 795–810. https://doi.org/10.1080/15583058.2019.1568615

Francioli, M., Petrini, F., Olmati, P., & Bontempi, F. (2021). Robustness of reinforced concrete frames against blast-induced progressive collapse. *Vibration, 4*, 722–742. https://doi.org/10.3390/vibration4030040

GSA. (2013). *Alternate path analysis and design guidelines for progressive collapse resistance*. US General Services Administration.

GSA. (2016). *Alternate path analysis and design guidelines for progressive collapse resistance revision 1*. London: US General Services Administration.

Güllü, H., & Karabekmez, M. (2017). Effect of near-fault and far-fault earthquakes on a historical masonry mosque through 3D dynamic soil-structure interaction. *Engineering Structures, 152*, 465–492. https://doi.org/10.1016/j.engstruct.2017.09.031

Hou, J., & Song, L. (2016). Progressive collapse resistance of RC frames under a side column removal scenario: The mechanism explained. *International Journal of Concrete Structures and Materials, 10*, 237–247. https://doi.org/10.1007/s40069-016-0134-y

Ikki, N., & Kiyomiya, O. (1996). Effect of axial concrete stress on bond strength of deformed bar. *Proceedings of Japan Concrete Institute, 21*, 373–378.

Ikki, N., Kiyomiya, O., & Yamada, M. (1996). Experimental study on the effects of numerous factors on bond-slip relationship. *Journal of Materials, Concrete Structures and Pavements, 33*, 73–83.

Jarernprasert, S., Bazan-Zurita, E., & Bielak, J. (2013). Seismic soil-structure interaction response of inelastic structures. *Soil Dynamics and Earthquake Engineering, 47*, 132–143. https://doi.org/10.1016/j.soildyn.2012.08.008

Jiang, J., Zhang, Q., Li, L., Chen, W., Ye, J., & Li, G. Q. (2020). Review on quantitative measures of robustness for building structures against disproportionate collapse. *International Journal of High-Rise Buildings, 9*, 127–154. https://doi.org/10.21022/IJHRB.2020.9.2.127

Kai, Q., Zhang, X. D., Fu, F., & Li, B. (2019). Progressive collapse resisting mechanisms of planar prestressed concrete frame. *ACI Structural Journal, 116*, 77–90. https://doi.org/10.14359/51715567

Karapetrou, S. T., Fotopoulou, S. D., & Pitilakis, K. D. (2015). Seismic vulnerability assessment of high-rise non-ductile RC buildings considering soil–structure interaction effects. *Soil Dynamics and Earthquake Engineering, 73*, 42–57. https://doi.org/10.1016/j.soildyn.2015.02.016

Khatibinia, M., Fadaee, M. J., Salajegheh, J., & Salajegheh, E. (2013). Seismic reliability assessment of RC structures including soil–structure interaction using wavelet weighted least squares support vector machine. *Reliability Engineering & System Safety, 110*, 22–33. https://doi.org/10.1016/j.ress.2012.09.006

Kheyroddin, A., Sharbatdar, M. K., & Farahani, A. (2019). Effect of structural height on the location of key element in progressive collapse of RC structures. *Civil Engineering Infrastructures Journal., 52*, 41–58. https://doi.org/10.22059/CEIJ.2019.247588.1449

Kiakojouri, F., De Biagi, V., Chiaia, B., & Sheidaii, M. R. (2020). Progressive collapse of framed building structures: Current knowledge and future prospects. *Engineering Structures, 206*, 110061. https://doi.org/10.1016/j.engstruct.2019.110061

Kiakojouri, F., Sheidaii, M. R., De Biagi, V., & Chiaia, B. (2021). Progressive collapse of structures: A discussion on annotated nomenclature. *Structures, 29*, 1417–1423. https://doi.org/10.1016/j.istruc.2020.12.006

Kim, J., & Choi, H. (2015). Monotonic loading tests of RC beam-column subassemblage strengthened to prevent progressive collapse. *International Journal of Concrete Structures and Materials, 9*, 401–413. https://doi.org/10.1007/s40069-015-0119-2

Kwon, K., & Kim, J. (2014). Progressive collapse and seismic performance of twisted diagrid buildings. *International Journal of High-Rise Buildings, 3*(3), 223–230. https://doi.org/10.21022/IJHRB.2014.3.3.223

Li, M., Lu, X., Lu, X., & Ye, L. (2014). Influence of soil-structure interaction on seismic collapse resistance of super-tall buildings. *Journal of Rock Mechanics and Geotechnical Engineering, 6*, 477–485. https://doi.org/10.1016/j.jrmge.2014.04.006

Li, S., Shan, S., Zhai, C., & Xie, L. (2016). Experimental and numerical study on progressive collapse process of RC frames with full-height infill walls. *Engineering Failure Analysis, 59*, 57–68. https://doi.org/10.1016/j.engfailanal.2015.11.020

Lin, K., Chen, Z., Li, Y., & Lu, X. (2022). Uncertainty analysis on progressive collapse of RC frame structures under dynamic column removal scenarios. *Journal of Building Engineering, 46*, 103811. https://doi.org/10.1016/j.jobe.2021.103811

Liu, X., Tang, Y., Lu, Z., Huang, H., Tong, X., & Ma, J. (2018). ESMD-based stability analysis in the progressive collapse of a building model: A case study of a reinforced concrete frame-shear wall model. *Measurement, 120*, 34–42. https://doi.org/10.1016/j.measurement.2018.01.038

Lysmer, J., & Kuhlemeyer, R. L. (1969). Finite dynamic model for infinite media. *Journal of the Engineering Mechanics Division*. https://doi.org/10.1061/JMCEA3.0001144

Mander, J. B., Priestley, M. J. N., & Park, R. (1988). Theoretical stress-strain model for confined concrete. *Journal of Structural Engineering, 114*, 1804–1826. https://doi.org/10.1061/(ASCE)0733-9445(1988)114:8(1804)

Marjanishvili, S. M. (2004). Progressive analysis procedure for progressive collapse. *Journal of Performance of Constructed Facilities, ASCE, 18*, 79–85. https://doi.org/10.1061/(ASCE)0887-3828(2004)18:2(79)

Martinez-Rueda, J. E., & Elnashai, A. S. (1997). Confined concrete model under cyclic load. *Materials and Structures, 30*, 139–147. https://doi.org/10.1007/BF02486385

Masoero, E., Wittel, F. K., Herrmann, H. J., & Chiaia, B. M. (2010). Progressive collapse mechanisms of brittle and ductile framed structures. *Journal of*

Engineering Mechanics, 136, 987–995. https://doi.org/10.1061/(ASCE)EM.1943-7889.0000143

Mello, L., Le, J. L., & Ballarini, R. (2020). Numerical modeling of delayed progressive collapse of reinforced concrete structures. *Journal of Engineering Mechanics, 146*, 1–11. https://doi.org/10.1061/(ASCE)EM.1943-7889.0001843

Mourlas, C., Khabele, N., Bark, H. A., Karamitros, D., Taddei, F., Markou, G., & Papadrakakis, M. (2020). Effect of soil–structure interaction on nonlinear dynamic response of reinforced concrete structures. *International Journal of Structural Stability and Dynamics, 20*, 2041013. https://doi.org/10.1142/S0219455420410138

Mucedero, G., Brunesi, E., & Parisi, F. (2020). Nonlinear material modelling for fibre-based progressive collapse analysis of RC framed buildings. *Engineering Failure Analysis, 118*, 104901. https://doi.org/10.1016/j.engfailanal.2020.104901

Panahi, S., & Zahrai, S. M. (2021). Performance of typical plan concrete buildings under progressive collapse. *Structures, 31*, 1163–1172. https://doi.org/10.1016/j.istruc.2021.02.045

Patel, B. R., & Shah, B. J. (2017). Progressive collapse assessment of reinforced concrete frame structure with and without considering actual soil condition. *Kalpa Pubations in Civil Engineering., 1*, 1–12. https://doi.org/10.29007/p792

Payganeh, M., & Mortezaei, A. (2020). Seismic damage assessment of RC buildings subjected to the rotational ground motion records considering soil-structure interaction. *Journal of Rehabilitation in Civil Engineering, 8*, 62–80. https://doi.org/10.22075/jrce.2019.17206.1319

Petrone, F., Shan, L., & Kunnath, S. K. (2016). Modeling of RC frame buildings for progressive collapse analysis. *International Journal of Concrete Structures and Materials, 10*, 1–13. https://doi.org/10.1007/s40069-016-0126-y

Pitilakis, D., & Clouteau, D. (2010). Equivalent linear substructure approximation of soil-foundation-structure interaction: Model presentation and validation. *Bulletin of Earthquake Engineering, 8*, 257–282. https://doi.org/10.1007/s10518-009-9128-3

Qian, K., Geng, S. Y., Liang, S. L., Fu, F., & Yu, J. (2022). Effects of loading regimes on the structural behavior of RC beam-column sub-assemblages against disproportionate collapse. *Engineering Structures, 251*, 113470. https://doi.org/10.1016/j.engstruct.2021.113470

Qian, K., Lan, D. Q., Li, S. K., & Fu, F. (2021). Effects of infill walls on load resistance of multi-story RC frames to mitigate progressive collapse. *Structures, 33*, 2534–2545. https://doi.org/10.1016/j.istruc.2021.06.015

Rahmani, A., Taiebat, M., Liam Finn, W. D., & Ventura, C. E. (2016). Evaluation of substructuring method for seismic soil-structure interaction analysis of bridges. *Soil Dynamics and Earthquake Engineering, 90*, 112–127. https://doi.org/10.1016/j.soildyn.2016.08.013

Rashidian, O., Abbasnia, R., Ahmadi, R., & Mohajeri Nav, F. (2016). Progressive collapse of exterior reinforced concrete beam-column sub-assemblages: Considering the effects of a transverse frame. *International Journal of Concrete Structures and Materials, 10*, 479–497. https://doi.org/10.1007/s40069-016-0167-2

Ren, P., Li, Y., Guan, H., & Lu, X. (2015). Progressive collapse resistance of two typical high-rise RC frame shear wall structures. *Journal of Performance of Constructed Facilities, 29*, 1–9. https://doi.org/10.1061/(ASCE)CF.1943-5509.0000593

Russell, J. M., Sagaseta, J., Cormie, D., & Jones, A. E. K. (2019). Historical review of prescriptive design rules for robustness after the collapse of Ronan Point. *Structures, 20*, 365–373. https://doi.org/10.1016/j.istruc.2019.04.011

Scalvenzi, M., & Parisi, F. (2021). Progressive collapse capacity of a gravity-load designed RC building partially collapsed during structural retrofitting. *Engineering Failure Analysis, 121*, 105164. https://doi.org/10.1016/j.engfailanal.2020.105164

Seffen, K. A. (2008). Progressive collapse of the World Trade Center: Simple analysis. *Journal of Engineering Mechanics, 134*, 125–132. https://doi.org/10.1061/(ASCE)0733-9399(2008)134:2(125)

Shayanfar, M. A., & Javidan, M. M. (2017). Progressive collapse-resisting mechanisms and robustness of RC frame–shear wall structures. *Journal of Performance of Constructed Facilities, 31*, 1–12. https://doi.org/10.1061/(ASCE)CF.1943-5509.0001012

Sivaselvan, M.V., & Reinhorn, A.M. (1999). Hysteretic models for cyclic behavior of deteriorating inelastic structures. Technical Report MCEER-99–0018.

Stafford Smith, B., & Coull, A. (1991). *Tall building structures; analysis and design*. Wiley.

Tao, Y., & Huang, Y. (2022). Numerical investigation on progressive collapse resistance of post-tensioned precast concrete beam-column assemblies under a column-loss scenario. *Engineering Structures, 251*, 113528. https://doi.org/10.1016/j.engstruct.2021.113528

Thomson, E. D., Perdomo, M. E., Picon, R., Marante, M. E., & Florez-Lopez, J. (2009). Simplified model for damage in squat RC shear walls. *Engineering Structures, 31*, 2215–2223.

Trapani, F. D., Giordano, L., & Mancini, G. (2020). Progressive collapse response of reinforced concrete frame structures with masonry infills. *Journal of Engineering Mechanics, 146*, 1–19. https://doi.org/10.1061/(ASCE)EM.1943-7889.0001723

Wolf, J. (1985). *Dynamic soil-structure interaction*. Electro Watt Engineering Services Ltd, prentice-hall, INC, Englewood cliffs, N.J.07632.

Yi, W. J., Yi, F., & Zhou, Y. (2021). Experimental studies on progressive collapse behavior of RC frame structures: Advances and future needs. *International Journal of Concrete Structures and Materials, 15*, 1–23. https://doi.org/10.1186/s40069-021-00469-6

Publisher's Note